An overview of Alpine and Mediterranean palaeogeography, terrestrial ecosystems and climate history during MIS 3 with focus on the Middle to Upper Palaeolithic transition

An overview of Alpine and Mediterranean palaeogeography, terrestrial ecosystems and climate history during MIS 3 with focus on the Middle to Upper Palaeolithic transition

Federica Badino[a,b,*], Roberta Pini[b], Cesare Ravazzi[b], Davide Margaritora[b], Simona Arrighi[a,c,d], Eugenio Bortolini[a], Carla Figus[a], Biagio Giaccio[b], Federico Lugli[a,e], Giulia Marciani[a,d], Giovanni Monegato[f], Adriana Moroni[c], Fabio Negrino[g], Gregorio Oxilia[a], Marco Peresani[h], Matteo Romandini[a,h], Annamaria Ronchitelli[c], Enza E. Spinapolice[i], Andrea Zerboni[j], Stefano Benazzi[a,k]

[a] Dipartimento di Beni Culturali, Università di Bologna, 48121 Ravenna, Italy

[b] C.N.R. - Istituto di Geologia Ambientale e Geoingegneria, 20126 Milano, Italy

[c] Dipartimento di Scienze Fisiche della Terra e dell'Ambiente, Università di Siena, 53100 Siena, Italy

[d] Centro Studi sul Quaternario, 52037 Sansepolcro, Italy

[e] Dipartimento di Scienze Chimiche e Geologiche, Università di Modena e Reggio Emilia, 41125 Modena, Italy

[f] C.N.R. - Istituto di Geoscienze e Georisorse, 35131 Padova, Italy

[g] Dipartimento Antichità, Filosofia e Storia, Università di Genova, 16126 Genova, Italy

[h] Dipartimento di Studi Umanistici, Sezione di Scienze Preistoriche e Antropologiche, Università di Ferrara, 44100 Ferrara, Italy

[i] Dipartimento di Scienze dell'Antichità, Università Sapienza, 00185 Roma, Italy

[j] Dipartimento di Scienze della Terra "A. Desio", Università degli Studi di Milano, 20133 Milano, Italy

[k] Department of Human Evolution Max Planck Institute for Evolutionary Anthropology, 04103 Leipzig, Germany

* Corresponding author: Federica Badino federica.badino@unibo.it

Università di Bologna

Dipartimento di Beni Culturali

Via degli Ariani 1

48121 Ravenna (Italy)

http://www.erc-success.eu/

Abstract

This paper summarizes the current state of knowledge about the millennial scale climate variability characterizing Marine Isotope Stage 3 (MIS 3) in S-Europe and the Mediterranean area and its effects on terrestrial ecosystems. The sequence of Dansgaard-Oeschger events, as recorded by Greenland ice cores and recognizable in isotope profiles from speleothems and high-resolution palaeoecological records, led to dramatic variations in glacier extent and sea level configuration with major impacts on the physiography and vegetation patterns, both latitudinally and altitudinally. The recurrent succession of (open) woodlands, including temperate taxa, and grasslands with xerophytic elements, have been tentatively correlated to GIs in Greenland ice cores. Concerning colder phases, the Greenland Stadials (GSs) related to Heinrich events (HEs) appear to have a more pronounced effect than other GSs on woodland withdrawal and xerophytes expansion. Notably, GS 9-HE4 phase corresponds to the most severe reduction of tree cover in a number of Mediterranean records. On a long-term scale, a reduction/opening of forests throughout MIS 3 started from Greenland Interstadials (GIs) 14/ 13 (ca. 55-48 ka), showing a maximum in woodland density. At that time, natural environments were favourable for Anatomically Modern Humans (AMHs) to migrate from Africa into Europe as documented by industries associated with modern hominin remains in the Levant. Afterwards, a variety

of early Upper Palaeolithic cultures emerged (e.g., Uluzzian and Proto-Aurignacian). In this chronostratigraphic framework, attention is paid to the Campanian Ignimbrite tephra marker, as a pivotal tool for deciphering and correlating several temporal-spatial issues crucial for understanding the interaction between AMHs and Neandertals at the time of the Middle to Upper Palaeolithic transition.

Keywords: Middle Upper Palaeolithic, Palaeoecology, Palaeoclimate, Marine Isotope Stage 3, Terrestrial records

1 Introduction

Climate variability and landscape transformations underlie the complex interaction between natural resources and human dynamics. The understanding of these changes over time relies on palaeoclimate and palaeoecological information obtained from different natural archives (e.g. terrestrial and marine sediments, speleothems, ice cores, etc.), which are well known for their potential to record even abrupt and high frequencies events. The Marine Isotope Stage 3 (MIS 3) in the Last Glacial Period (Lisiecki and Raymo, 2005) is one of the most highly unstable phases, as far as climate is concerned, closely interwoven with the recent human evolution history. MIS 3 (ca. 60-30 ka) was characterized by major rapid climatic changes showing high variability, associated with abrupt atmospheric shifts over Greenland (Dansgaard-Oeschger [D-O] events) and episodes of massive iceberg discharge into the North Atlantic (Heinrich events [HEs]),

enhancing cold and dry conditions at mid-to-low latitudes (Fletcher and Sánchez Goñi, 2008; Fleitmann et al., 2009; Naughton et al., 2009; Fletcher et al., 2010a).

Within this context, the Middle to Upper Palaeolithic transition (ca. 50-30 ka in Europe and western Asia, Higham et al. 2014; Benazzi et al., 2015; Hublin 2015; Douka and Higham, 2017; Been et al., 2017; Margherita et al., 2017) represents one of the pivotal phases in human evolution documenting the demise of the autochthonous Neandertals and their replacement by Anatomically Modern Humans (AMHs). Many authors suggest that the eastern Mediterranean region and, in turn, the Italian Peninsula, served as gateways for the immigration and spread of AMHs from Africa to western Eurasia (van Andel et al., 2003; Müller et al., 2011; Moroni et al., 2013; 2018), where various transitional technocomplexes (eg., the Uluzzian in Italy and Greece, the Châtelperronian in central and south western France and northern Spain, the Neronian in south eastern France) replaced pre-existing Mousterian cultures (Mellars, 2006). Neandertals and AMHs societies developed in a context of continuous climatic fluctuations between cold-arid (Greenland Stadial, GS) and mild-humid (Greenland Interstadial, GI) conditions (Staubwasser et al., 2018). Surprisingly, despite the apparent body adaptations to live under rigid climates conditions (Steegmann et al., 2002), e.g., a wide and tall nasal aperture useful in humidifying and warming cold and dry air (Franciscus, 1999; Wroe et al., 2018), Neandertals did not survive into the coldest phases of MIS 3. Their extinction is statistically placed around 40 ka cal BP (Higham et al., 2014) and almost in coincidence with Greenland Stadial 9/HE 4, which is a noticeable cold phase recorded in both marine and terrestrial records (e.g. Fedele et al, 2003; Guellevic et al., 2014 and references therein). Several hypotheses have been proposed about Neandertal extinction and AMHs

93 replacement, and the debate is still unresolved (e.g., Mellars 2006; Hoffecker 2009;
94 Benazzi et al., 2011; 2015; Villa and Roebroeks, 2014; Higham et al., 2014; Hublin, 2015;
95 Rey-Rodríguez et al., 2016; Greenbaum et al., 2018).

96 To disentangle the role played by climate, ecosystem changes and physiography in such
97 human processes, a palaeoclimate and palaeoecological perspective focusing on Europe
98 and the Mediterranean area is essential. These efforts represent part of a wider interest in
99 determining how abrupt climate changes modified past environments.

100 The aim of this paper is to present the state-of-the-art of palaeoclimate and
101 palaeoecological researches relevant to the ERC Consolidator Grant 2016 "SUCCESS -
102 *The earliest migration of Homo sapiens in southern Europe: understanding the biocultural*
103 *processes that define our uniqueness*". To contribute to the discussion about the arrival of
104 AMHs in Southern Europe, the pattern of their diffusion and their interactions with
105 Neandertals, a review of the current knowledge about the climate context and the
106 landscape structure is presented. A selection of high-resolution palaeoecological records
107 covering the time span between HE 5 to 3, known for their strong impact in western
108 Eurasia, are discussed to explore the effects of short-term climate variability on
109 ecosystems and human interactions.

110

2 Reference climate records for the Last Glacial period and signal synchronicity between different realms

2.1 MIS 3 as recorded in Greenland ice cores

MIS 3, which lasted from 60 ka to 30 ka, was characterized by millennial-scale climate oscillations commonly referred to as Dansgaard-Oeschger (D-O) events. These events, particularly well-defined in Greenland ice cores, were first described by Dansgaard et al. (1993). Typically, D-O events are featured by an abrupt transition (within a few decades) from a cold phase (GS), into a warm phase (GI). NGRIP, GRIP and GISP2 ice cores provide master records for these rapid climatic changes throughout the Last Glacial cycle (MIS 5d to the end of MIS 2; ca. 116–11.7 ka) in the North Atlantic region (McManus et al., 1999). Boundaries between GS and GI periods were established based on both stable-oxygen isotope ratios of the ice ($\delta^{18}O$, reflecting mainly local temperature) and calcium ion concentrations ($[Ca^{2+}]$ reflecting mainly atmospheric dust loading) measured in the ice (**Fig. 1, a-c**) (Rasmussen et al., 2014). The close timing of $\delta^{18}O$ and $[Ca^{2+}]$ abrupt shifts is also indicative of reorganizations in atmospheric circulation (Steffensen et al., 2008). Notably, $[Ca^{2+}]$ data reflect primarily changes in dust concentration but also changes in dust source conditions and transport paths (Fischer et al., 2007a, 2007b). During D-O events North Atlantic region temperature and East Asian storminess were tightly coupled and changed synchronously with no systematic lead or lag (Ruth et al., 2007), thus providing instantaneous climatic feedback. This relationship was stable over the entire Last Glacial period.

According to Petersen et al. (2013), the driving mechanism of GI onset is linked to the rapid collapse of an ice-shelf fringing Greenland, potentially due to subsurface warming.

During GI, a gradual cooling controlled by the timing of ice-shelf regrowth leads to GS conditions that lasted for centuries up to millennia. NGRIP temperature reconstructions based on $\delta^{15}N$ isotope measurements (**Fig. 1, b**) show T increase at the onset of each GI ranging from 6.5 °C (D-O 9) up to 16.5 °C (D-O 11), with an uncertainty of ±3 °C (Kindler et al., 2014).

A recent important step forward is represented by the development of the ice-core GICC05 chronology (Andersen et al., 2006; Rasmussen et al., 2006; Svensson et al., 2008; Seierstad et al., 2014) and its flow model-based extension (GICC05modelext) published in Rasmussen et al. (2014), which allowed to achieve a reference template for the pattern of climate variability during the Last Glacial cycle.

2.2 Climate signals in mid- to low-latitude marine records

A well-known feature in North Atlantic marine sediments is the presence of coarse sediment layers, i.e. the ice-rafted debris (IRD, Ruddiman, 1977). Such depositional episodes, known as Heinrich Events (HE), are related to massive discharge, rafting and melting of icebergs into the ocean and the consequent fall of detrital sediments trapped in the ice on the ocean floor (Heinrich, 1988) and unambiguously identified during GS phases of the Last Glacial period (e.g. Bond et al., 1992; 1993; Hemming 2004).

It is widely assumed that D-O events and HE are linked to reorganisations and/or variations in the strength of the Atlantic Meridional Overturning Circulation (AMOC) (Broecker et al., 1990). Specifically, Bagniewski et al. (2017) suggest a 30-50% weakening of the AMOC during GSs and a complete shutdown during HEs, also coinciding with large increases in the abundance of foraminifer polar species (e.g. *N. pachyderma*, **Fig. 1, h-g**).

The Iberian Margin (**Fig.1**) is a key area for the reconstruction of these dynamics thanks to its distal position, i.e. outside of the main belt of ice rafting, which limit disturbance of the sediments (Bard et al., 2000; Pailler and Bard, 2002). The recently obtained Sea Surface Temperature (SST) curve based on the biomarker TEX^{H}_{86} in MD95-2042 core (Darfeuill et al., 2016) highlights that the greater cooling peaks occurred during HEs (about 3-5 °C; **Fig. 1, f**). This feature is in disagreement with the general pattern emerging over Greenland, where temperatures reconstructed during GS are roughly comparable and show more stable values to each other (**Fig. 1, b**). In addition, Martrat et al. (2007) argue that SST changes occur a few centuries before the subsequent generation of icebergs, which are traced by increases in IRD percentage. Regarding this issue, various studies state that HEs are shorter (Roche et al., 2004; Peters et al., 2008) than the corresponding GS and occur after the AMOC entered a weakening trend (Flückiger et al., 2006; Marcott et al., 2011). Thus, HEs seem to be a consequence rather than the cause of the AMOC weakening (e.g., Alvarez-Solas et al., 2010, 2013; Marcott et al., 2011; Barker et al., 2015).

Given the uncertainty across the North Atlantic in the ocean reservoir correction (e.g., Stern and Lisiecki, 2013; Butzin et al., 2017), and the lack of a clear HE signature in the $\delta^{18}O$ Greenland isotopic record (Rasmussen et al., 2014), it is difficult to establish where HEs lie exactly within the D-O framework (Andrews and Voelker, 2018). Indeed, Rasmussen et al. (2014) did not designate the temporal positions of HEs. However, new Greenland ice cores proxy records (e.g., ^{17}O-excess; **Fig. 1, d**) are linked to a lower-latitude hydrological cycle signal (Guillevic et al., 2014). This might help in the future to

better constrain HE in the ice core series, allow exploring time leads and lags in between events happening at different latitudes.

2.3 Synchronicity between abrupt Greenland events and terrestrial responses in Southern Europe

Over the last two decades, the INTIMATE project (INTegrating Ice-core, MArine, and TErrestrial records; e.g., Blockley et al., 2012; Rasmussen et al., 2014) has proposed a series of event-stratigraphic templates based on the isotopic and dust concentration changes in Greenland ice cores. The alternating pattern of stadial and interstadial geologic-climatic units, due to their very high stratigraphic and temporal resolution and precise dating, constitute the most comprehensive and best resolved archive of high-frequency climate variability. The Northern-Hemisphere transmission of such millennial-scale signals (reflected in $\delta^{18}O$ variations) depends on the extremely rapid atmospheric circulation changes (probable lag a couple of years only; Rasmussen et al., 2014). These changes are induced by migration of the Polar Front (PF) and shifts of the Intertropical Convergence Zone (ITCZ) at mid-to-low-latitudes (Europe and the Mediterranean areas) (e.g., Peterson and Haug, 2006), which in turn induce atmospheric circulation and local rainfall changes.

Problems in synchronization of MIS 3 records mainly arise from the uncertainties of the age models, based on different dating methods, the intrinsic difficulties in dating these events, in particular for those intervals at or beyond the limit of the radiocarbon technique (see section 7.1) and the scarcity of precisely dated and unambiguously synchronous

stratigraphic events, such as tephra layers, magnetic excursions and cosmogenic nuclide peaks. Speleothems are excellent archives for recording these abrupt isotopic changes (e.g., Fleitmann et al., 2009; Moseley et al. 2014; Weber et al., 2018), since they are among the most accurately datable archives, i.e., within the last ca 100 ka, two sigma (95%) errors can be below 1% of the U/Th age. Their deposition is predominantly influenced by either temperature (higher latitude) or precipitation (lower latitude), but both ultimately linked to Northern Hemisphere temperature fluctuations (e.g., McDermott, 2004; Genty et al., 2006). In general, speleothem records unambiguously show the signature of D-O cycles and HEs on European and Mediterranean climate, and a millennial to sub-millennial scale synchronicity in climatic shifts between European and Greenland isotopic records. Despite a generally continuous calcite deposition during the GI 14-GI 13 interval, even at the elevation of the modern snowline in the Alps (Spötl and Mangini, 2007; Moseley et al., 2014), their registration is often fragmentary and hiatuses may have occurred during cold/dry phases (i.e. HE 5 and HE 4; Spötl et al., 2002; Moseley e al. 2014, **Fig. 1, e;** Weber et al., 2018). In fact, ITCZ variations may have also affected local rainfall patterns, triggering enhanced dryness notably in the Mediterranean (Fletcher and Sánchez Goñi et al., 2008; Fleitmann et al., 2009). However, precise determination of the durations of these hiatuses may provide valuable information about climatic thresholds that affect regional climatic conditions (Moreno et al., 2010; Zhornyak et al., 2011; Stoll et al., 2013). Overall, the climatic pattern underlying these $\delta^{18}O$ profiles during MIS 3 strongly resembles that of Greenland ice cores at millennial scales, and in many cases corresponding to the detail of decadal-scale cooling events within interstadials (Moseley et al., 2014).

3 Reference mid-to-high resolution MIS 3 palaeoecological records in Southern Europe and in the Mediterranean region

Palaeoecological and palaeoclimate archives considered in this review paper (**Tab. 1**) are mostly located in Southern Europe and in the Mediterranean region between ca. 36° and 46.5° N throughout the Atlantic, Continental, Alpine, and Mediterranean biogeographical regions (**Fig. 2**; European Environment Agency, 2016). A few others dataset from central Europe accompany these sites. Selected records (i) cover a relevant interval during the ca. 30 – 60 ka time-frame, (ii) are mostly characterized by a sub-millennial/multi-decadal time resolution (see **Tab. 1**), and (iii) include quantitative or semi-quantitative geochemical (i.e., stable isotopes) and/or vegetation (i.e. palynological data) climate proxy variables. Most of them are placed in the Mediterranean region, which borders the Atlantic region in the west and the western Eurasian sub-continental region including both the Black Sea and the Anatolian regions (**Fig. 2**). The latter area is of particular interest because it possibly served as a gateway for the spread of AMHs into Europe (Müller et al., 2011). Thus, palaeoclimatic and palaeoecological information from these sites are of great importance and serve as background for the archaeological work in the Levant.

239

Site	Archive type	Latitude (decimal degrees)	Longitude (decimal degrees)	Elevation (m asl)	Interval/Time period (ka)	Palaeoenvironmental /climate proxies	Mean temporal resolution for MIS 3 (yrs/sample)	References
TERRESTRIAL								
Abric Romani (Spain)	Carbonate sediments/ travertine deposits	41.53	1.68	310	41-70 ka	Palynological data	200 yrs	*Burjachs et al., 2012*
Azzano Decimo (Italy)	Lake sediments	45.85	12.9	10	0-215 ka (discontinuous)	Palynological data	1150 yrs	*Pini et al., 2009*
Lac du Bouchet (France)	Lake sediments	44.83	3.82	1200	ca. 8-120 ka	Palynological data	ca. 1000 yrs	*Reille and Beaulieu, 1990*
Eifel maar (Germany)	Lake sediments	50.16	6.85	420	0-60 ka	Palynological data	Decadal/centennial	*Sirocko et al., 2016*
Fimon (Italy)	Lake sediments	45.46	11.53	23	27-138 ka	Palynological data	960 yrs	*Pini et al., 2010*
Füramoos (Germany)	Peat deposits	47.98	9.88	662	0-14 ka, 40-140 ka	Palynological data	ca. 900-1200 yrs	*Müller et al., 2003*
Ioannina 284 (Greece)	Lake sediments	39.75	20.85	470	0-132 ka	Palynological data	325 yrs	*Tzedakis et al., 2002*
La Grand Pile (France)	Lake sediments	47.73	6.50	330	0-140 ka	Palynological data	ca. 250 yrs	*Woillard 1978; Guiot et al., 1992*

Lagaccione (Italy)	Lake sediments	42.57	11.8	355	4-100 ka	Palynological data	420 yrs	*Magri, 1999*
Les Echets (France)	Lake sediments	45.9	4.93	267	ca. 10-75 ka	Palynological data	ca. 500 yrs	*Beaulieu and Reille, 1984*
Kopais K-93 (Greece)	Lake sediments	38.43	23.05	95	10-130 ka	Palynological data	830 yrs	*Tzedakis, 1999*
Megali Limni (Greece)	Lake sediments	39.1	26.32	323	22-62 ka	Palynological data	150 yrs	*Margari et al., 2009*
Lago Grande di Monticchio (Italy)	Lake sediments	40.93	15.62	656	0-132 ka	Palynological data	210 yrs	*Allen et al. 1999; Wutke et al., 2015*
Ohrid (Republic of Macedonia and Albania)	Lake sediments	40.91	20.67	693	0-500 ka	Palynological data	ca. 850 yrs	*Sadori et al. 2016*
Prespa (Republic of Macedonia, Albania and Greece)	Lake sediments	40.95	20.96	849	0-92 ka	Palynological data	ca. 1070 yrs	*Panagiotopoulos et al. 2014*
Ribains (France)	Lake sediments	44.83	3.82	1075	10-150 ka	Palynological data	ca. 1500 yrs	*Beaulieu and Reille, 1992b*
Tenaghi Phillippon (TF II) (Greece)	Peat-dominated succession	41.17	24.33	40	0-130 ka	Palynological data	120 yrs	*Wijmstra 1969; Müller et al., 2011; Wulf et al., 2018*

Valle di Castiglione (Italy)	Lake sediments	41.88	12.77	44	0-250 ka	Palynological data	440 yrs	*Follieri et al., 1988-1998*
Lago di Vico (Italy)	Lake sediments	42.32	12.28	507	0-90 ka	Palynological data	ca. 500 yrs	*Leroy et al., 1996; Magri and Sadori, 1999.*
Bunker cave - Bu2 (Germany)	Speleothems	51.36	7.6	184	From 52 to 50.9 ka and from 47.3 to 42.8 ka	Calcite $\delta^{18}O$, $\delta^{13}C$	decadal/ multidecadal-scale	*Weber et al., 2018*
Hölloch cave (Höl-7, Höl-16, Höl-17, and Höl-18) - NALSP (Germany)	Speleothems	47.38	10.15	1240–1438	35-65 ka (discontinuous)	Calcite $\delta^{18}O$, $\delta^{13}C$	decadal/ multidecadal-scale	*Mosely et al., 2014*
Kleegruben cave - SPA 49 (Austria)	Speleothems	47.09	11.67	2165	46-58 ka	Calcite $\delta^{18}O$, $\delta^{13}C$	decadal/ multidecadal-scale	*Spötl et al., 2002*
Soreq cave (Israel)	Speleothems	31.7	35	400	0-60 ka	Calcite $\delta^{18}O$, $\delta^{13}C$	40 yrs	*Bar-Matthews et al., 1999-2000*
Villars cave - Vil 27 (France)	Speleothems	45.3	0.5	175	30-55 ka	Calcite $\delta^{18}O$, $\delta^{13}C$)	53 yrs (between 48.5 and 40.5 ka) and 203 yrs (between 40.5 and 30 ka)	*Genty et al., 2010*

Villars cave - Vil 9 (France)	Speleothems	45.3	0.5	175	32-83 ka (discontinuous)	Calcite $\delta^{18}O$, $\delta^{13}C$	91 yrs (between 51.8 and 40.4 ka) and 195 yrs (between 40.4 and 31.8 ka)	*Genty et al., 2003*
Villars cave - Vil 14 (France)	Speleothems	45.3	0.5	175	29-52 ka	Calcite $\delta^{18}O$, $\delta^{13}C$	81 yrs (between 52.2 and 41.7 ka) and 1066 yrs (between 41.7 and 28.9 ka)	*Wainer et al., 2009*
NGRIP (Greenland)	Ice core	75.1	42.32	2917	8-120 ka	$\delta^{18}O$; calcium ion concentration data ([Ca2+])	re-sampled to 20-year resolution	*Seierstad et al., 2014; Rasmussen et al., 2014*
MARINE								
MD04-2845 (Western France)	Marine sediments	45.35	-5.22	-4100	30-140 ka	Palynological data; Foraminiferal $\delta^{18}O$; Ice-rafted debris record	540 yrs	*Sánchez Goñi et al., 2008*
MD95-2042 (Iberian margin)	Marine sediments	37.8	-10.17	-3148	27-138 ka	Palynological data; Foraminiferal $\delta^{18}O$; Ice-rafted debris record; $U^{k'}_{37}$ and TEX_{86} biomarkers (SST)	ca. 370 yrs	*Sánchez Goñi et al., 1999-2000-2008-2009*

MD95-2043 (Alboran sea)	Marine sediments	36.13	-2.62	-1841	0-50 ka	Palynological data; Foraminiferal $\delta^{18}O$; C_{37} Alchenones (SST)	260 yrs	*Cacho et al., 1999; Sánchez Goñi et al., 1999; Fletcher and Sánchez Goñi, 2008*
LC21 (Aegean sea)	Marine sediments	35.66	26.58	-1522	0-160 ka	Foraminiferal $\delta^{18}O$	ca. 200 yrs	*Grant et al., 2012*
ODP 976 (Alboran sea)	Marine sediments	36.20	-4.30	-1108	>1Ma	Palynological data; Foraminiferal $\delta^{18}O$	Ranging between 50 and 200 yrs	*Combourieu-Nebout et al., 2002; Combourieu-Nebout et al., 2009; Genty et al., 2010*

Tab. 1 List of selected sites from S-Europe and the Mediterranean area that entirely or partially cover the MIS 3 chronological framework, specifying location, available vegetation-climate proxy variables and time resolution. References to published data are also indicated

3.1 Vegetation response to D-O events and HEs in Southern Europe and Mediterranean region

The history of vegetation during MIS 3 in Southern Europe and in the Mediterranean area relies on several palaeoecological studies carried out in lake and peat stratigraphic sequences. In **Fig. 3** we consider the evidence for millennial-scale variability and long-term vegetation trends from selected records covering the period between ca. 60 - 30 ka (i.e., GI 17 to GI 5). The records are presented on the most recent chronology available for each one. On the whole, this data shows a high sensitivity of vegetation response to D-O events, making South Eastern Europe and the Italian Peninsula a key geographical area for high-resolution palaeoenvironmental researches during the last glacial period.

In southern Europe, the recurrent succession of (open) woodlands, including temperate taxa, and grasslands with xerophytic elements (**Fig. 3**), have been tentatively correlated to GIs in Greenland ice cores (Fletcher et al., 2010b). This assumption is reasonable for this geographic area as thermophilous trees persisted in refugia and appeared to have expanded rapidly during each interstadial without substantial migration lags (Harrison and Sánchez Goñi, 2010).

Investigations at Lago Grande di Monticchio (Allen et al., 1999, 2000) were the first to provide an independently dated Late Pleistocene palaeoenvironmental record, due to its varved sequence. Furthermore, the identification of known tephra layers, one of which is the Campanian Ignimbrite (CI), has also been used to improve the age-depth model (Wutke et al., 2015). The high-resolution pollen record (ca. 200 yrs/sample) obtained from

the Monticchio core reveals millennial-scale changes in woody/open environments throughout MIS 3. Palaeoecological data indicate an alternation between cold/dry steppic vegetation, referred to GS periods, and an increased range of woody taxa including deciduous *Quercus*, *Abies* and *Fagus* (up to 30–60% AP), referred to GI periods (Allen et al., 1999; Fletcher et al., 2010b). Similarly, other long pollen records from volcanic lakes in central and southern Italy, i.e., Lagaccione and Valle di Castiglione (**Fig. 3**; Follieri et al., 1988, 1998; Magri, 1999), show remarkable changes of vegetation composition, structure and biomass including millennial-scale fluctuations in forest development with deciduous and evergreen *Quercus, Corylus, Fagus*, *Betula* and *Picea* (Fletcher et al., 2010b). The lower temporal resolution of these latter records (ca. 400 yr/sample) in turn reduced the chances to precisely identify each GI (**Fig. 3**).

In northern Italy, pollen records from Lake Fimon (**Fig. 3**) and Azzano Decimo (Pini et al., 2009; Pini et al., 2010) indicate phases of conifer-dominated forest expansion (*Pinus sylvestris-mugo* and *Picea*), rich in cool broad-leaved trees (*Alnus* cf*. incana* and tree *Betula*) and accompanied by a reduced warm-temperate component (*Tilia*). In both records, individual D–O events cannot be identified due to the low temporal resolution (ca. 800-1000 yr/sample), nevertheless the well-documented long vegetation trend is indicative of a persistent afforestation. In fact, only moderate forest withdrawals occurred and some temperate trees (e.g., *Tilia* and *Abies*) persisted up to ca. 40 ka BP (Pini et al., 2010). Interestingly, peaks of *Tilia* pollen were found (Cattani and Renault-Miskowski, 1983-84) in layers preserving Mousterian artefacts and dated to 40.6-46.4 ^{14}C ka in the cave sediments at the Broion shelter (Leonardi and Broglio, 1966), and also in Paina cave inter-pleniglacial deposits (Bartolomei et al., 1987-88; Cattani 1990).

At southern latitudes, high-resolution pollen records from Ioannina, Tenaghi Philippon and Megali Limni (Greece, **Fig. 2** and **Fig. 3;** Wijmstra, 1969; Tzedakis et al., 2006; Margari et al., 2009; Müller et al., 2011; Wulf et al., 2018,) show exceptional series of millennial and sub-millennial vegetation changes correlated to a number of GI/GS (Fletcher et al. 2010b; Pross et al. 2015). Concerning colder phases, the GSs related to HEs appear to have a more pronounced effect than other GSs on woodland withdrawal and xerophytes expansion. Notably, GS 9-HE 4 phase corresponds to the most severe reduction of tree cover in a number of records (e.g., Megali Limni, Tenaghi Philippon, Valle di Castiglione and Ioannina; **Fig. 3**). Interestingly, pollen records from different bioclimatic areas seem to show differences in terms of magnitude of the response to cold events due to local ecosystem structures. In sites where moisture availability was not a limiting factor, differences in the magnitude of climate forcing during HEs seem to be well expressed in terms of major vegetation changes (e.g., Ioannina, Monticchio) (**Fig. 3**). However, where temperate tree populations were near their tolerance limit, the environmental stress associated with HEs probably crossed a critical threshold resulting in large population contraction with an almost complete drop in forest cover (i.e., Tenaghi Philippon, Megali Limni) (Tzedakis et al., 2004) (**Fig. 3**).

On a long-term scale, a reduction/opening of forests throughout MIS 3 (see **Fig. 3**) took place from GI 14, showing a maximum in woodland density, to the following GI 12 and GI 8. During GI 14/ 13 interval, conditions were notably humid and mild in the eastern Mediterranean as indicated by the Soreq cave isotopic record (Bar-Matthews et al., 2000) and also over Europe (Allen et al.,1999; Sánchez Goñi et al., 2002; Fletcher et al., 2010b).

Despite the relatively high amount of palaeoecological information for southern Europe, the spatial distribution of records in this heterogeneous geographic sector remains uneven. Such differences in the expression of millennial-scale events suggest that site characteristics need to be taken into account when mapping the spatial patterns of changes and trying to elucidate the mechanisms involved. New records are needed (e.g., from northern and southern Italy, Turkey, the Levant), in order to refine the knowledge of eco-climatic gradients across the continent and to better understand regional vegetation patterns.

3.2 Fire dynamics in Southern Europe and Mediterranean region

High-resolution microcharcoal records can provide new insights to understand fire-vegetation dynamics in relation to climate variability (e.g. D-O cyclicity/HE events) and/or human activities (e.g., Whitlock and Larsen, 2001; Iglesias et al., 2015). As for the Last Glacial period, few microcharcoal records are available from terrestrial (e.g., Magri, 2008; Margari et al., 2009; Pini et al., 2009, 2010) and marine records (e.g., Daniau et al., 2007, 2009). **Fig. 3** shows microcharcoal data for some Southern East European terrestrial sites: Lake Fimon, Valle di Castiglione, Lagaccione and Megali Limni (MIS 3 partially documented).

Overall, a fire regime variability mainly associated with fluctuations in forest cover occurred between GS (lower fire activity) and GI (higher fire activity). Higher microcharcoal concentration during periods of afforestation suggests enhanced fire activity favoured by increasing woody fuel and biomass accumulation during GI (Magri, 1994), as observed also by Daniau et al. (2007; 2009) for southwestern Iberia (MD95-2042 and MD04-2845 cores, **Fig. 2**). Contrary to this pattern, NE-Italy experienced isolated major fire episodes

over a generally low-intensity fire regime; at Lake Fimon (Pini et al., 2010; **Fig. 2**) the strongest fire episode of the whole Late Pleistocene record is coeval to a drop in forest cover mirrored by steppe expansion, possibly correlated to HE4 (**Fig. 3**). Since the palaeoecological data from this site suggest relatively high moisture availability during MIS 3 (Pini et al., 2010), such climatic context may have prevented long-term fire activity south of the Alps, despite biomass availability. This evidence indicates that the incidence of fires is not always directly correlated with the degree of afforestation. This framework supports a regional climatic influence on fire regimes over SE-Europe with a direct climatic control on fuel availability during the Last Glacial period.

4 Snapshots of European palaeogeography and ecoclimatic zones during GI 12 and the LGM

With the aim of setting Palaeolithic humans in a palaeoenvironmental scenario, we chose two MIS 3-2 key intervals relevant for the human evolution and marking paleoclimate extreme conditions: the GI 12 and LGM. We plotted the main European palaeogeography and palaeoecology landscape features on geographical snapshots (**Figure 4A and B**). In detail, GI 12 snapshot (ca. 46.8 to 44.2 ka according to Rassmussen et al., 2014) represents a phase of major forest expansion during MIS 3 also coincident with the AMHs arrival in Europe (Grotta del Cavallo, ca. 45.5 ka; Benazzi et al., 2011; Zanchetta et al., 2018) (**Figure 4A).** The second one spans the time interval of both the SIS (Scandinavian Ice Sheet) and the European mountain glacier culminations during the LGM (26 to 21 ka cal BP in Europe, see Hughes et al., 2016; Monegato et al., 2017), which was characterized by one of the most pronounced forest contractions of MIS 3-2 time span

(**Figure 4B**). From GI 12 to LGM, climate changes led to dramatic variations in glacier extent and sea level with major impacts on the physiography of mountain areas, coastal regions and the hydrologic systems. The latter two are also known for their important role in AMHs dispersal into Europe (Mellars, 2006; Hublin, 2014).

4.1 Palaeoenvironmental setting during Greenland Interstadial 12 (MIS 3)

4.1.1. Reconstructed gradients ecogeography within eco-climatic zones

We reconstructed terrestrial ecosystems for a time frame corresponding to GI 12 (**Fig. 4A**) by combining palaeobotanical records (for Central Europe: see Van Meerbeeck et al., 2011 and references therein; Follieri et al., 1988; Beaulieu and Reille, 1992a-b; Drescher-Schneider et al., 2007; for Mediterranean Europe: Magri, 1999; Sánchez Goñi et al., 2002 and 2009; Pini et al., 2009, 2010; Müller et al., 2011) and ecoclimatic gradients. These gradients rely both on large scale latitudinal zones (i.e., Tundra zone and Forest-tundra zone, and related positions of polar timberline, see Holtmeier,1985; Archibold, 2012), spanning the northern half of European subcontinent and on regional elevational mountain belts in southern Europe (see Fig. 4A). We assumed GI 12 and GI 14 vegetation peaks to have been similar at the same site, although GI 12 was shorter, and used both GI 14 and GI 12 data to implement our reference dataset. Fossil data was improved by (a) elevational ecoclimatic relationships and (b) vegetation models (Alfano et al., 2003). However, available gridded vegetation models do not account for vegetation distribution in complex mountain regions that actually represent 75% (total areas above 500 m altitude obtained from GIS elaboration) of the southern European landscape. Indeed, elevation gradients can be very steep and, within a 1-km^2 grid cell, elevation can vary up to, or even more than, 500 m. In these contexts, forests display a characteristic discontinuity in their

379 distribution with a main boundary representing the upper limit of forest canopies
380 associated with temperature decrease along elevational gradients. Thus, some
381 inaccuracies in the vegetation distribution can be expected in global models due to the
382 coarse spatial resolution of climate datasets that can be affected by errors in the local
383 temperature estimation (i.e., more than 1°C for a lapse rate of about −0.5°C/100 m).

384 A number of ecoclimatic zones are featured by distinct regional climates (i.e. coniferous
385 and broad-leaved woodlands along the northern coast of Portugal and Spain; map of the
386 European Environment Agency, 2015). Within each zone, local climates (i.e. mountain
387 areas) have been qualified by elevational gradients of orographic precipitation. The main
388 features of these altitudinal gradients are the upper timberline limit and the glacier
389 Equilibrium Line Altitude. Given the determinants of the warmest month temperature
390 (TJuly) on the upper timberline, caused by heat deficiency (Tranquillini, 1979; Jobbagy and
391 Jackson, 2000; Körner and Paulsen, 2004), we used TJuly reconstructions for GI 12 to
392 estimate the altitude of montane timberline. In order to moderate the effects of CO_2
393 changes on plant fertilization (Farquhar, 1997), we included past timberlines as calibration
394 test of our estimations. The timberline position in the Italian Central Alps during the
395 Bølling-Allerød (1700-1800 m asl: Tinner et al., 1999; Ravazzi et al., 2007) is a good test
396 as the GI 1 is the only D-O interstadial which occurred under moderately low CO_2
397 concentration; furthermore, relevant fossil records are relatively common as they were not
398 erased by LGM glacier activity. Given the position of the alpine timberline during the
399 Bølling-Allerød and the associated pollen-based mean TJuly (18,5-19°C; Vallè et al.,
400 unpublished data), we infer the timberline position during GI12 using the difference
401 between TJuly for GI12 (ca. 18°C) and the Bølling-Allerød. This difference was projected

over an elevational gradient using an average environmental lapse rate of about -0,67°C/100 m (Furlanetto et al., 2019), to obtain an historical timberline for GI 12 (ca. 1600 m in the Italian Central Alps). The method was also tentatively applied to estimate timberlines in the Mediterranean region. Here, however, many boreal tree species were missing during MIS 3, thus ecophysiological requirements of Mediterranean timberline species were considered.

4.1.2. Estimating Equilibrium Line Altitudes of mountain glaciers

By using elevational lapse rates we also estimated the Equilibrium Line Altitude (ELA) position during GI12 in the Central Alps (Vallé et al., unpublished data). Again, temperature differences between the LGM ELA positions (e.g. Kuhlemann et al. 2008; Hughes and Woodward, 2016) and GI 12 were projected over elevational gradients and tested against the temperatures and ELA related to the Egesen stage, Younger Dryas (Kelly et al., 2004; Ivy-Ochs et al., 2008; Delmas, 2015; Ruszkiczay-Rüdiger et al., 2016; Popescu et al., 2017; Gromig et al., 2018). The results of a recent Parallel Ice Sheet Model (PISM) with climate forcing deriving from WorldClim and the ERA-Interim reanalysis (Seguinot et al., 2018) proved to fit our results for the Central Alps (GI 12 ELA 2100 m, 626 m higher than the LGM ELA). As a best approximation, the same value was added to the LGM ELA position for the Pyrenees, Balkans and Carpathians, providing a GI12 reconstructed ELA of ca. 2400 m, ca. 2100 m and 2000 m, respectively.

4.1.3. The GI 12 palaeoenvironmental map

European vegetation gradients were particularly strong during the major interstadial phases (i.e., spanning about 2000-2500 years), characterized by large arboreal excursions

both latitudinally and altitudinally, north and south of the Alps. The GI 12 is one of these key representative warm intervals. In **Figure 4A,** we depict the palaeoenvironmental setting of mid and southern Europe (between 52° and 35° latitude N) during GI 12. It is also shown a reconstruction of the coastline: -74 m a.s.l. (Waelbroeck et al., 2002; Antonioli, 2012). A substantial seashore enlargement over Europe led to increased connectivity, especially between the Italian peninsula and the Western Balkans region, between Mediterranean islands, and also the emergence of large areas north of the Black Sea and in the North Sea (**Fig. 4A**). The Scandinavian Ice Sheet (SIS), which grew during MIS 4, had almost entirely melted at mid MIS 3 (60–45 ka) (Lambeck et al., 2010; Wohlfarth, 2010).

We summarize hereafter the main constrains of the featured ecoclimatic zones.

Forest tundra ecozone. The northern timberline was given as the northern limit of the forest tundra mosaic (*sensu* Walter and Breckle, 1986; Holtmeier, 2009; Van Meerbeeck et al., 2011). The abundance of gleysols with charred wood dated to around 45 ka at the base of loess-luvisol sequences in Central and Eastern Europe (Haesaerts et al., 2009; Moine et al., 2017) supports locating the zonoecotone of forest tundra for wetter interstadial phases of MIS 3 between 47° and 52° - 54° N, i.e. north of the Alps (Fig. 2A). The geography of northern timberline in Central and Eastern Europe was drawn according to modelling results by Alfano et al. (2003). In the forest tundra zonoecotone, the forest is found mainly in warmer and drier places, with stunted individuals at the waterlogging edaphic ecotone.

445 **Atlantic zone.** This biogeographical region closely interacts with the northeast Atlantic
446 Ocean margin. Expansion of Atlantic forests with *Betula, Pinus* and deciduous *Quercus* is
447 recorded during GI 12 and 14, probably reflecting obliquity forcing at higher latitudes
448 (Sánchez Goñi et al., 2008). Vegetation in Western Iberia also responded immediately
449 (within the resolution of the record) to SST changes on millennial time scales during MIS 3.
450 Increases in temperatures offshore translated to increased tree cover on land and vice
451 versa. This rapid response to interstadials warming supports the idea that thermophilous
452 taxa persisted in NW-Iberian refugia throughout the last glacial period (Roucoux et al.,
453 2005).

454 **Iberian region.** Average annual precipitation map for the Iberian peninsula (years 1901-
455 2009; Schneider et al., 2014) depicts a strong gradient from the north-western to northern
456 Atlantic coasts (1100 - 1500 mm/year) to central Spain and Mediterranean areas (250 -
457 700 mm/year). During GI 12, humid Atlantic air masses promoted higher moisture
458 availability on the northern coasts of Portugal and Spain, which could support the
459 occurrence of open temperate woodlands. In the inner Iberian areas, grasslands occupied
460 drier lowlands; increasing afforestation was visible along altitudinal gradients.

461 **Adriatic and Tyrrhenian Basins.** Lowering of the sea led to the emergence of a wide
462 area north of the 44° parallel in the Adriatic sea. The area hosted terrestrial vegetation,
463 from mixed conifer and broad-leaved woodlands in the inner Friulian-Venetian Plain to
464 more open communities and then grasslands, the latter building a wide belt along the
465 coastal margins. Differences in the humidity regimes between the eastern Adriatic and the
466 western Tyrrhenian Basins bordering Italy are responsible for the asymmetry of

ecosystems represented in Fig. 2A. Palaeoecological records from the Tyrrhenian coast suggest almost persistent moisture availability during MIS 3. Similar to the current situation, it can be assumed that precipitation was mainly generated by the orographic uplift of air charged with moisture from the Tyrrhenian Sea.

Balkans and Aegean regions: During GI 12, terrestrial ecosystems were dominated by open temperate woodland and/or temperate forest-steppe south of 40°N, with increasing amount of trees north of this latitude. At lower altitudes, in wider belts bordering the eastern Adriatic, Ionian and eastern Mediterranean Seas, grasslands developed.

Central Anatolian plateau. In the Anatolian region the reconstructed historical GI 12 timberline is located at 1500 m asl. Areas down to 500-800 m could support open forest vegetation, especially along the Turkish coasts of the Black Sea, characterized by a temperate oceanic climate with the greatest amount of precipitation of the whole region (Turkish State Meteorological Service, 2006). Moisture does not reach inland areas; inner plateau bordered by the Pontic Mountains to the north and the Taurus to the south is characterized by a continental climate with strongly contrasting seasons. During GI12, in these inner areas open grasslands expanded.

A reconstruction of European vegetation patterns during a warm/moist phase of MIS3 was proposed by van Andel and Tzedakis (1998). The vegetation subdivisions provided in this early reconstruction largely overlap with the picture of terrestrial ecosystems provided in our Fig. 2A, with some differences **(i)** the reconstruction of van Andel and Tzedakis (1998) is plotted on a simplified sketch map of Europe not taking into account the altitudinal gradients, indeed represented on our GIS topographic base. This is important as far as

489 temperature and moisture gradients play an important role in determining both latitudinally
490 and altitudinally extents of vegetation belts; **(ii)** minor differences between the two
491 reconstructions are visible in the shape of the limit of the northern timberline (between 53-
492 55°N in Fig. 2A - based on Alfano et al., 2003; around 50°N according to van Andel and
493 Tzedakis, 1998); **(iii)** Fig. 2A provides indication on ELA and timberline positions during an
494 interstadial, thanks to data from papers published in recent years and quantitative climate
495 reconstructions for the last glacial cycle.

496 **4.2 Palaeogeography of Southern and Central Europe during LGM**

497 We attempted a LGM palaeogeographical reconstruction of mid-southern Europe in order
498 to allow direct comparison of physical patterns between GI 12 (i.e. a major interstadial
499 within MIS 3) and the subsequent LGM (i.e. 30 to 16.5 ka cal BP, Lambeck et al., 2014)
500 cold phase. For this map, we chose to represent the physical geography of Europe during
501 the time interval spanning both the SIS and the European mountain glacier culminations
502 (26 to 21 ka cal BP in Europe, see Hughes et al., 2016; Monegato et al., 2017). At this
503 time, main climatic patterns can be displayed though different climate zones according to
504 Köppen-Geiger classification (Becker et al., 2015).

505 The SIS passed the coast of western Norway at the time of the Laschamp palaeomagnetic
506 excursion (ca. 41 ka) (Valen et al., 1995; Mangerud et al., 2010). At ca. 21 ka the ice-sheet
507 attained its maximum extent (**Fig. 4 B**; Hughes et al., 2016). During this period the
508 European Alps were extensively covered by an ice-dome which generated valley glaciers.
509 In the Alps, the maximum ice extent was reached during the LGM around 25 ka, when
510 large piedmont glaciers advanced onto the Alpine foreland. This is well constrained by the
511 end-moraine systems, in which the LGM moraines were dated (radiocarbon, OSL and

cosmogenic nuclide surface exposure dating methods) and point to large ice lobes at the outlet of major valleys (e.g., Monegato et al., 2007, 2017; Ivy-Ochs et al., 2008, 2018; Ravazzi et al., 2012; Reber et al., 2014; Salcher et al., 2015). In the south-western and in the eastern sectors many valley glaciers remained confined within the valley (e.g., Jorda et al., 2000; Bavec and Verbic, 2011; Rossato et al., 2013, 2018; Federici et al., 2016), as testified by the reconstruction of LGM moraines. In the fringe area of the Alpine chain many isolated small ice caps or mountain glaciers developed without merging with the major trunk glaciers (e.g., Carraro and Sauro, 1979; Forno et al., 2010; Monegato, 2012). Large outwash megafans developed from the front of the Alpine glaciers or from the funnelling of outwash streams in the lower reach of the valleys (Fontana et al., 2014). By this time, large glaciers developed in the Pyrenees and many frontal moraines were dated (Delmas, 2015 and references therein); here glaciers mostly remained confined within the valleys and several small and isolated glaciers occurred (e.g., Pallas et al., 2010). Other small glacier systems were present in the Iberian mountains; these advances had different age development, from 31 to 20 ka, according to Oliva et al. (2019) compilation. Documented ice-caps in the French Massif Central (de Gôer, 1972) and in the Vosges (Seret et al., 1990), but chronology on glacial landforms needs to be improved (Buoncristiani and Campy, 2004).

Valley glaciers spread in the Carpathians and Tatra ranges (e.g., Ehlers et al., 2011; Makos et al., 2018). Their size were reconstructed on the basis of remote sensing and field analyses (Zasadni and Klapyta, 2014) and the age of their maximum spread is constrained with exposure dating at about 25 ka (Engel et al., 2015; Makos et al., 2018).

534 The Balkan Peninsula was deeply studied in the last decay (see Hughes and Woodward,
535 2016 for a review). Therein, mountain glaciers developed in a karstic environment with
536 specific characteristics (Adamson et al., 2014; Zebre and Stepisnik, 2015; Zebre et al.,
537 2016). Most of the outwash system into the karstic network and the outwash fans were
538 very confined and limited to the basins where glaciers flowed (Zebre et al., 2016, 2019).
539 Also small glaciers formed on the highest mountain chains of the Apennines (e.g., Giraudi
540 and Giaccio, 2016; Baroni et al., 2018; Mariani et al., 2018).

541 The region surrounding the Adriatic lowstand plain collected the drainage from Alpine
542 outwash systems and from the surrounding Apennine and Balkan rivers, which had
543 important karst underground flows. The large Adriatic lowstand delta (**Fig. 4B**; Maselli et
544 al., 2014; Pellegrini et al., 2015) accreted as sea level fell down to -120 m or -149 m
545 (Antonioli and Vai, 2004).

546 Late Pleistocene aeolian sediments are widespread in Europe (e.g. Haase et al., 2007;
547 **Fig. 4B**) and they represent further indicators of past environmental changes. Loess is
548 commonly distributed in Central, Eastern, and Southern Europe (e.g., Kukla, 1975;
549 Smalley and Leach, 1978; Frechen et al., 1997; Haase et al., 2007; Cremaschi et al.,
550 2015; Marković et al., 2015; Terhorst et al., 2015; Zerboni et al., 2018); in the
551 Mediterranean region loess bodies formed also along the present day coastline (Chiesa et
552 al., 1990; Cremaschi, 1990; Wacha et al., 2011a,b; Boretto et al., 2017). Loess is generally
553 associated with glacial environmental conditions, with dry and cool climate and increased
554 wind strength (Pye, 1995). In continental Europe and in the Mediterranean basin
555 Pleistocene loess accumulated in mid-continental plains free of ice sheets, at the margins
556 of mountain ranges, along the shorelines of the Mediterranean and at the semi-arid

margins of the Sahara and Levantine deserts (Obruchev, 1914; Cremaschi, 1990; Haase et al., 2007; Crouvi et al., 2010; Lindner et al., 2017; Lehmkuhl et al., 2018 a,b; Zerboni et al., 2018). In Mediterranean Europe, as in the Po Plain, major loess sources are the outwash plains fed by glaciers flowing from mountains (Alps and Apennines) (Cremaschi,1990). Loess deposition occurred during most of the Quaternary glacials and was related to a general decrease in forest cover and expansion of semideserts, steppe, and treeless environments (Rousseau et al., 2018). Notwithstanding many efforts in establishing fine MIS 4 to 2 loess chronology with luminescence methods and stratigraphic correlations (e.g., Timar et al., 2010; Timar-Gabor et al., 2011; Thiel et al., 2014) due to intrinsic properties of loess and to the possible occurrence of sedimentary gaps (Thiel et al., 2014), the resolution of loess studies is still lower than those of other continental archives. Likely, Late Pleistocene loess sedimentation occurred, at least, since the end of MIS4 and during MIS 3 and 2 (Marković et al., 2015; Terhorst et al., 2015). In Italy, loess sedimentation is recorded along the margins of the Po Plain and discontinuously along the shorelines of the Mediterranean, where loess is better preserved within rockshelters (Cremaschi, 2004; Peresani et al., 2008). Italian loess dates back to the Late Pleistocene and mostly formed since the end of MIS 4 (Cremaschi, 1990, 2004); but loess deposits occur as well in sections that contain Mousterian artifacts dating to MIS 3 (e.g., Cremaschi, 1990; Cremaschi et al., 2015; Zerboni et al., 2015; Delpiano et al., 2019). More recently, a few loess bodies have been dated also to MIS 2 (Ferraro, 2009; Zerboni et al., 2015), showing a good continuity in wind sedimentation in the Late Pleistocene, at least at the northern margin of the Po Plain. Italian loess is often interlayered by paleosols, allowing the identification of less arid phases. For instance, at the Val Sorda section a chernozem-like palaeosoil, has been dated at ca. 27 ka BP (Ferraro et al., 2009); whereas at Monte

Netto site moderate pedogenesis (including clay illuviation) compatible with forest cover occurred at times between 44 and 25 ka BP (Zerboni et al., 2015).

5 Focus on spatial vegetation response in Italy during MIS 3

The pie charts presented in **Fig. 5** show long-term vegetation dynamics and geographic patterns in Italy between ca. 30 and 60 ka cal BP using data from privileged sites (North to South): Lake Fimon, Lagaccione, Valle di Castiglione and Monticchio. For each record, selected pollen taxa are consistently grouped according to their ecology and climate preferences in order to facilitate their comparison (for further information see caption and legend in **Fig. 5**).

A higher forest cover in Northern Italy compared to Mediterranean sites is an unchanged background feature during MIS 3. Indeed, the glaciated Alps must have represented a very sharp rainfall boundary leading to more humid conditions in south-eastern alpine foreland persistently forested and a northern treeless boreal and continental landscape, as shown by La Grande Pile, Les Echets and Füramoos pollen records (**Fig. 2**; Woillard, 1978; Beaulieu and Reille, 1984; Guiot et al., 1992; Müller et al., 2003). The palaeoecological record from Lake Fimon documents a mosaic of boreal forests dominated by *Pinus sylvestris/mugo* over the 60 to 30 ka cal BP time period. However, a continuous xerophytic steppe expansion (e.g. *Artemisia* and Chenopodiaceae), coupled with the reduction of temperate elements (deciduous *Quercus* and other thermophilous taxa) in favour of pine woodlands, notably since 40-45 ka, suggests a shift towards drier/colder conditions possibly enhanced by GS 9-HE 4 phase.

602 The contraction of temperate forests is also recorded throughout MIS 3 in central Italy
603 (Lagaccione and Valle di Castiglione) and southern Italy at Lago Grande di Monticchio. In
604 these sites, open forests dominated by deciduous *Quercus*, *Corylus, Fagus, Tilia, Ulmus*
605 and *Carpinus betulus* experienced their maximum expansion between ca. 60-45 ka.
606 Afterwards, open environments (*Artemisia*-dominated steppe/ wooded steppe) expanded
607 between 45-30 ka (**Fig. 5**).

608 This general overview suggests latitudinal (and also altitudinal) climatic patterns and
609 rainfall gradients along the Italian peninsula due to its complex physiographic structure (i.e.
610 the presence of two high mountain ranges, Alps and Apennines), to be taken into account
611 when reconstructing past vegetation dynamics as it has already been shown for Greece
612 (Tzedakis et al., 2004).

613

614 ## 6 Archaeological framework

615 During the first half of MIS 3, and particularly during GIs 14/13 ca. 55-48 ka, natural
616 environments were favourable for AMHs to migrate from Africa into Europe (Müller et al.,
617 2011). The scenario of an initial AMHs movement into Europe is supported by industries
618 associated with modern hominin remains found in few excavated localities: Üçağızlı cave
619 (Turkey) (Güleç et al., 2002; Kuhn et al., 2009); Ksar Akil (Lebanon) (Copeland and
620 Yazbeck, 2002; Yazbeck, 2004; Douka et al., 2013); Manot cave (Israel) (Hershkovitz et
621 al., 2015). Around 45 to 39 ka, Neandertals were replaced by AMHs (Higham et al., 2014),
622 and a variety of early Upper Palaeolithic cultures emerged (e.g., Uluzzian and Proto-

623 Aurignacian in the central-eastern Mediterranean regions; see Arrighi et al. and Marciani et
624 al., this issue).

625 The cultural complex known as Uluzzian has been attested in the Italian Peninsula and
626 southern Balkans around 45-40 ka (**Fig. 6**; Palma di Cesnola, 1989; Ronchitelli et al.,
627 2009; Moroni et al., 2013; Peresani, 2014; Zanchetta et al., 2018). This techno-complex
628 was coeval with the arrival of AMHs in Europe as evidenced by the anatomical features of
629 two deciduous teeth discovered in Grotta del Cavallo in Apulia (Benazzi et al., 2011,
630 although challenged by Zilhão et al., 2015, and further discussed in Moroni et al., 2018).
631 Along the Italian Peninsula, the Uluzzian is currently best known in cave sedimentary
632 successions by its stratigraphic position above the Mousterian and under the Proto-
633 Aurignacian, when the latter is present, and also in several open-air sites (**Fig. 6**).
634 Recently, the Uluzzian has also been observed in northern Italian cave sites, expanding its
635 cultural borders from what was thought to be exclusively central-southern after the
636 discovery of assemblages at Grotta Fumane and at the Riparo Broion shelter (Peresani,
637 2008; Peresani et al., 2016, 2018). Other sites in the Adriatic-Ionian region exhibit
638 Uluzzian elements (Crvena Stijena; Mihailović et al., 2017; Klissoura Cave; Starkovich,
639 2017; Kephalari; Darlas and Psathi, 2016), opening new perspectives in looking at the
640 appearance and spread of the Uluzzian over the entire area of the Adriatic basin.

641 In several sites from the Middle to Upper Palaeolithic transition is documented by the
642 Proto-Aurignacian technocomplex. The available chronological framework indicates a
643 Proto-Aurignacian occupation ending with the Campanian Ignimbrite eruption in Southern
644 Italian Castelcivita (Gambassini, 1997) and Serino sites (Lowe et al., 2012; Wood et al.,
645 2012). However, this tephrostratigraphic marker also constrains the end of the Uluzzian

techno-complexes at Grotta del Cavallo on the Ionic coast of Salento (Lecce) (Zanchetta et al., 2018; section 7.2). In N-W Italy, the earliest Proto-Aurignacian is that of the Balzi Rossi sites complex in the region of Liguria (NW Italy), where it has been identified at Riparo Mochi and Riparo Bombrini sites (Douka et al., 2012; Riel-Salvatore and Negrino, 2018). At these sites, the main outlines of the industry remain stable beyond the end of GS9/HE4 (Riel-Salvatore and Negrino, 2018), comparably to Grotta Fumane in the north of Italy (Falcucci et al., 2017; Falcucci and Peresani, 2018). The assessment of these temporal-spatial issues and new chronological information are fundamental for understanding the dynamics of the cultural and ecological-anthropological changes that occurred in S-Europe at the Middle to Upper Palaeolithic transition.

Already before 43 ka, very early Aurignacian assemblages, reflecting an initial AMHs advance into central Europe, have also been found along the Danube (Willendorf II, Lower Austria; Nigst et al., 2014), suggesting the Danube's role as a spatial corridor for human dispersal in the Early Upper Palaeolithic (e.g., Floss, 2003; Hussain and Floss, 2016). A similar role is hypothesized for the Don River system near the Black Sea (Anikovich et al., 2007). Beside large river systems, also coastal plains played a relevant role channelling AMHs dispersal into Europe (Mellars, 2006; Hublin, 2014). The close similarity between the available dates for the early AMH arrival in the Mediterranean and in Germany on the Danube, might suggest a rapid access in Europe via two routes, along both the Danube corridor and the Mediterranean coasts (Douka et al., 2012).

7 Chronological issues

7.1 Difficulties in dating the Middle to Upper Palaeolithic transition

Building reliable radiocarbon chronologies for sequences covering time intervals beyond and/or close to the limit of the radiocarbon technique (i.e., ca. 50 ka) remain challenging. Indeed, the low levels of residual ^{14}C activity induces lower precision (higher uncertainty) and accuracy (higher offset of the measured isotope ratio with respect to the actual one) of AMS measurements and makes samples much more vulnerable to contamination (e.g., Bird et al., 1999; Higham, 2011; Wood, 2015). In old samples, due to the low ^{14}C content, even very negligible percentages of modern carbon give very high contamination levels leading to wholly distorted chronologies, with resulting ages that can be younger of several millennia (Higham et al., 2009; Higham, 2011). Indeed, this makes the dating of small amounts of ancient carbon, i.e., more prone to contamination, even more challenging (e.g., Bird et al., 2014). Such problems can be partially overcome in long, continuous sedimentary succession that are biostratigraphically well-constrained using indirect approaches based on record alignment strategies, i.e., one record on a depth-scale is aligned onto a “dated reference” record (Govin et al., 2015); provided that the underlying assumptions, i.e., recognition of the events and their one-to-one correlation, are reasonably demonstrated. Yet, whenever possible, tephra markers and/or relative chronologies based on varved sediments can also be used to refine or validate age-models.

7.2 The Campanian Ignimbrite (CI) marker

The Campanian Ignimbrite (CI) super-eruption (southern Italy, $^{40}Ar/^{39}Ar$ age: 39.85 ± 0.14 ka, 2σ; ^{14}C age: 34.29 ± 0.09 ^{14}C ka BP, 1σ; Giaccio et al., 2017) produced the most

689 widespread tephra of western Eurasia, extending from the Tyrrhenian Sea to the Russian
690 Plain (e.g., Costa et al., 2012; Marti et al., 2016; **Fig. 7**). Its relevance as a key
691 chronological and stratigraphic marker for addressing a series of issues concerning the
692 European MIS 3 period – including the tempo and the palaeoecological factors involved in
693 the human bio-cultural evolution at the Middle-Upper Palaeolithic transition – has been
694 recognised long ago (e.g., Fedele et al., 2003) and eventually consolidated by a number of
695 papers: e.g., Giaccio et al., 2006 (see Higham et al., 2009 for the updated chronology of
696 Grotta Fumane); Pyle et al., 2006; Fedele et al., 2008; Giaccio et al., 2008; Hoffecker et
697 al., 2008; Lowe et al., 2012; Satow et al., 2015; Wutke et al., 2015; Wulf et al., 2018;
698 Zanchetta et al., 2018.

699 At several archaeological sites of the central Mediterranean, Balkans and Russian Plain
700 the CI tephra acts as a marker for the end of either final Mousterian with Uluzzian
701 elements (Crvena Stijena, Montenegro, Morley and Woodward, 2011; Mihajlovic and
702 Whallon, 2017), Uluzzian (Apulia region in southern-eastern Italy and Greece; e.g., Douka
703 et al., 2014; Zanchetta et al., 2018) or Proto-Aurignacian techocomplexes (e.g., Serino
704 open-air site and Castelcivita Cave in southern-western Italy and Kostenki site complex in
705 Russia; e.g., Giaccio et al., 2008 and references therein). However, although falling in its
706 dispersal area, the CI has not been detected at the Adriatic site of Grotta Paglicci (Apulia,
707 Southern Italy) and on the opposite Tyrrhenian side, at Grotta della Cala. In both caves the
708 Protoaurignacian seems to stretch beyond the CI event based on ^{14}C chronology (Paglicci)
709 and the studied materials (Marciani et al., this issue).

The CI tephra occurs in all the above-mentioned sites either as a relatively proximal, thick primary pyroclastic succession (e.g., Serino open-air site; Accorsi et al., 1978; Giaccio et al., 2006) or as a discrete layer, with a sharp lower contact with underling sediments, made of purely volcanic material (i.e., glass shards or pumice fragments with mineral accessories) with no or negligible contamination by clastic sediments. These features are consistent with a sub-primary (re)deposition of ash layers by the wind or run-off shortly after its emplacement as primary fallout along landforms nearby sheltered or open-air archaeological sites (e.g., Brunis et al., 2019). Specifically, at Castelcivita site, both Plinian pumice and co-ignimbritic ash layers are recorded in their eruptive stratigraphic order, suggesting that the two eruptive units were transported and redeposited in the cave immediately after their fall (fall and rolling process) (Giaccio et al., 2008; Giaccio et al., 2016). The sub-primary nature of the CI tephra, i.e., no appreciable time elapsed between CI tephra deposition and the eruption, is also supported by the available radiocarbon chronology of the archaeological layers immediately below CI tephra strata, which are statistically indistinguishable from the CI eruption age (Benazzi et al., 2011; Wood et al., 2012; Douka et al., 2014; Giaccio et al., 2017). On the whole, both radiocarbon chronology and CI tephra marker suggest that around 40 ka the central Mediterranean region was a cultural, and possibly biological, mosaic, suggesting the possible coeval occurrence of the final Mousterian (Crvena Stijena), Uluzzian (Apulia and Greece) and Protaurignacian lithic technocomplexes (Campania).

Particularly significant is also the climatostratigraphic position of the CI tephra as revealed by a number of marine and terrestrial palaeoclimatic records spread in the wide region of its dispersal area (**Fig. 7**). In this framework, the palaeoecological and tephrostratigraphic

high-resolution (120 yr/sample) record of Tenaghi Philippon (Greece, Wulf et., al 2018) offers the unique opportunity to compare the chronostratigraphic position of CI in relation to the palaeoenvironmental context at a centennial scale during the Middle to Upper Palaeolithic transition. In detail, CI deposition occurred ca. 1000 years after the onset of a phase of marked arboreal pollen drop corresponding to the GS 9 (ca. 40.58 cal ka BP) and 3280 years before the onset of GI8 (ca. 36.3 cal ka BP) (**Fig. 7**; Wulf et al., 2018). Similarly, at Monticchio site, the CI was deposited ca. 820 years after the onset of GS 9 (**Fig. 3**). However, at Tenaghi Philippon the resulting total duration of ca. 4280 years for GS 9 strongly deviates from the ca. 2000 years obtained at Lago Grande di Monticchio (Wutke et al., 2015) and from the 1680 years in the NGRIP record (i.e. from 39.90 to 38.22 ka GICC05; Rasmussen et al., 2014). A similar position is verified in number of other terrestrial and marine palaeoenvironmental records (e.g., Mediterranean and Black Sea marine records and Lake Ohrid, and Lesvos Island pollen profiles; see Giaccio et al., 2017 and references therein). Despite the general agreement in placing the CI well after the beginning of GS 9 (ca. 400 years, according to the alignment of records proposed in Giaccio et al., 2017), which is marked by a drop in arboreal pollen and temperate taxa (**Fig. 7)**, it seems that further investigations are needed to fully disentangle temporal discrepancies between records and to convincingly correlate the interval encompassing GI 8-10 to the D-O events. This is also challenging due to the inadequate resolution of most of the available pollen records if compared to the short GI 9 duration (i.e., 250-yr-long GICC05; Rasmussen et al., 2014), which only briefly interrupts the GS 10 to GS 9 interval representing over 4 millennia of cold stadial conditions.

With specific regards to these chronological issues, it is worth noting that the paired, high-precision, multiple $^{40}Ar/^{39}Ar$ and ^{14}C, ages for the CI revealed an offset of ca. 1 ka between the calendar age of the CI as determined by its direct $^{40}Ar/^{39}Ar$ dating and the calibrated ^{14}C age of the CI using IntCal13 calibration curve (Giaccio et al., 2017), thus highlighting the occurrence of a further source of uncertainty when comparing records whose age models are based on calibrated ^{14}C ages with others anchored to different time-scales (e.g., U/Th or Greenland ice chronology). This offset is now confirmed by a recent study, which reports a record of paired U/Th and ^{14}C ages from the Chinese Hulu Cave stalagmite, continuously spanning the last 54 ka (Cheng et al., 2018). This new record also reveals a radiocarbon plateau between ca. 37.5 ka and ca. 39.1 ka at ca. 33.5 ^{14}C ka BP that could have affected the age model of records based on ^{14}C chronology and thus be responsible for the above-mentioned notable age discrepancy in the length of the GS9 as recorded in different Mediterranean records. A distortion of the IntCal13 calibration curve at this time interval is also suggested by the recently published continuous record of the $\Delta^{14}C$ spanning between ca. 47.3 and 39.6 ka cal. BP from the Tenaghi Philippon lake succession (Staff et al., 2019).

All this information strictly related to this stratigraphic marker consolidate the notion of the CI as a pivotal tool for deciphering and evaluating the potential interconnection between climate, environmental, and human biological-cultural dynamics at the Middle to Upper Palaeolithic transition, as well as in disentangling several temporal-spatial issues, crucial for understanding the mechanisms underlying the interaction between AMHs and Neandertals.

8 Concluding remarks and future developments

In this review, we summarized the current state of knowledge, also contributing with new elaborations of available data, on climate history, terrestrial ecosystems and palaeogeography, with the main aim to place Neanderthals and AMHs in the context of MIS 3 European landscape. Neanderthals lived in Eurasia alongside anatomically modern humans until ca. 40 ka. This overlap suggests direct or indirect contacts between the two species on a European sub-continental scale, potentially leading to interbreeding and cultural exchanges (Higham et al., 2014). To decipher the possible implications of climate variability and palaeoenvironmental transformation in such human processes, including Neanderthals extinction, two main aspects must be kept in mind: (i) the millennial/sub-millennial terrestrial response to high-frequency climate variability resulted in a pronounced and rapid alternation between forested and more open environments. Interestingly, the most relevant tree cover reductions in southern Europe are correlated to HEs, notably GS9-HE4; (ii) a long-term climatic trend (i.e., between ca. 50 and 25 ka) that led to dramatic increasing of the glaciers extent and lowering of the sea level, with major impacts on the coast landscape and on physiography and vegetation patterns. This implied the progressive development of effective ecological and physiographic barriers (i.e. the Alpine ice-dome) that limited connections between continental and Mediterranean Europe. In contrast, the gradual enlargement of coastlines and reorganization of European river systems may have played a key role in the migration processes.

To better understand and integrate these aspects, within the ERC - SUCCESS project, a Work Package is specifically dedicated. Studies will concentrate on the time span between Heinrich Event 5 to 3, known for their strong impact in Mediterranean Europe, the Balkans

and Italy (Follieri et al., 1988; Allen et al., 2000; Lézine et al., 2010; Pini et al., 2010; Müller et al., 2011, Panagiotopoulos et al., 2014).

Attention will be paid to the reference record of Lake Fimon (Venetian Alpine foothills, north-eastern Italy). This area is indeed well-known as it provides both a Late Pleistocene palaeoecological record (Pini et al., 2010) and several Middle to Late Palaeolithic sites yielding evidence of Neandertal and AMH occupation (Grotta Fumane and Riparo Broion shelter; Peresani, 2011; **Fig. 3**). High-resolution palynostratigraphic researches are currently in progress on the Lake Fimon core will be matched with archaeological information from cave deposits in the same region to answer specific questions relevant to the ERC Project, i.e. the effects of climate variability on the environments of last Neandertals - early AMH, the role of fire, etc. Finally, to better comprehend regional vegetation patterns and eco-climatic gradients across the Italian peninsula, palaeoenvironmental proxies from Lake Fimon will be profitably compared to Central and Southern Italian records, through the elaboration of available series and the investigation of new sites.

Acknowledgements

This work was funded by ERC under the European Union's Horizon 2020 research and innovation programme (grant agreement No 724046 - SUCCESS); website: http://www.erc-success.eu/. Thanks are due to Prof. D. Haase, who kindly provided the shapefiles of loess distribution in Europe used in Fig. 4 B and to Prof. P.C. Tzedakis for

helpful comments on Fig. 4 A. We also thank three anonymous reviewers and the editor Dusan Boric for the valuable comments, which improved the quality of the manuscript.

References

Accorsi, C.A., Aiello, E., Bartolini, C., Castelletti l., Rodolfi, G., Ronchitelli A., 1978. Il giacimento paleolitico di Serino (Avellino): stratigrafia, ambienti e paletnologia. Atti della Società Toscana di Scienze Naturali, 86, 1979, 435-487.

Adamson, K.R., Woodward, J.C., Hughes, P.D., 2014. Glaciers and rivers: Pleistocene uncoupling in a Mediterranean mountain karst. Quaternary Science Reviews 94, 28–43.

Alfano, M.J, Barron, E.J., Pollard, D., Huntley, B., Allen, J.R.M., 2003. Comparison of climate model results with European vegetation and permafrost during oxygen isotope stage three. Quaternary Research, 59, 97-107.

Allen, J.R.M., Brandt, U., Brauer A., Hubberten, H.-W., Huntley B., Keller, J., Kraml, M., Mackensen, A., Mingram, J., Negendank, J.F.W., Nowaczyk, N.R., Oberhänsli, H., Watts, W.A., Wulf, S., Zolitschka, B., 1999. Rapid environmental changes in southern Europe during the last glacial period. Nature, 400, 740-743.

Allen, J.R.M., Watts, W.A., Huntley, B., 2000. Weichselian palynostratigraphy, palaeovegetation and palaeoenvironments; the record from Lago Grande di Monticchio, southern Italy. Quaternary International, 73/74, 91-110.

Alvarez-Solas, J., Charbit S., Ritz, C., Paillard, D., Ramstein, G., Dumas, C., 2010. Links between ocean temperature and iceberg discharge during Heinrich events. Nature Geoscience, 3, 122-126.

843 Alvarez-Solas, J., Robinson, A., Montoya, M., Ritz, C., 2013. Iceberg discharges of the last
844 glacial period driven by oceanic circulation changes. PNAS, 110 (41): 16350-16354.

845 Andersen, K.K., Svensson, A., Johnsen, S.J., Rasmussen, S.O., Bigler, M., Röthlisberger,
846 R., Ruth, U., Siggaard-Andersen, M.L., Steffensen, J.P., Dahl-Jensen, D., Vinther, B.M.,
847 Clausen, H.B., 2006. The Greenland Ice Core chronology 2005, 15–42 kyr. Part 1:
848 Constructing the time scale, Quaternary Science Reviews, 25, 3246–3257.

849 Andrews, J. T., Voelker, A.H., 2018. “Heinrich events” (& sediments): A history of
850 terminology and recommendations for future usage. Quaternary Science Reviews, 187,
851 31-40.

852 Anikovich, M. V., Sinitsyn, A. A., Hoffecker, J. F., Holliday, V. T., Popov, V. V., Lisitsyn, S.
853 N., Forman, S. L., Levkovskaya, G. M., Pospelova, G. A., Kuz’mina, I. E., Burova, N. D.,
854 Goldberg, P., Macphail, R. I., Giaccio B., Praslov, N. D., 2007. Early Upper Paleolithic in
855 Eastern Europe and implications for the dispersal of modern humans. Science, 315
856 (5809), 223-226.

857 Antonioli, F., Vai, G.B., 2004 (Eds.). Litho-palaeoenvironmental Maps of Italy During the
858 Last Two Climatic Extremes. Climex Maps Italy e Explanatory Notes. Bologna, p. 80.

859 Antonioli, F., 2012. Sea level change in western-central Mediterranean since 300 kyr:
860 comparing global sea level curves with observed data. Alpine and Mediterranean
861 Quaternary, 25 (1), 15-23.

862 Archibold, O. W., 2012. Ecology of world vegetation. Springer Science & Business Media.

863 Arrighi, S., Moroni, A., Tassoni, L., Boschin, F., Badino, F., Bortolini, E., Boscato, P.,
864 Crezzini, J., Figus, C., Forte, M., Lugli F., Marciani, G., Oxilia G., Negrino F., Riel-
865 Salvatore J., Romandini, M., Spinapolice, E. E., Peresani, M., Ronchitelli, A., Benazzi, S.,
866 this issue. Bone tools, ornaments and other unusual objects during the Middle to Upper
867 Palaeolithic transition in Italy.

868 Bagniewski, W., Meissner, K.J., Menviel, L., 2017. Exploring the oxygen isotope fingerprint
869 of Dansgaard-Oeschger variability and Heinrich events. Quaternary Science Reviews,
870 159, 1-14.

871 Barker, S., Chen, J., Gong, X., Jonkers, L., Knorr, G., Thornalley, D., 2015. Icebergs not
872 the trigger for North Atlantic cold events. Nature, 520, 333-336.

873 Baroni, C., Guidobaldi, G., Salvatore, M.C., Christl, M., Ivy-Ochs, S., 2018. Last glacial
874 maximum glaciers in the Northern Apennines reflect primarily the influence of southerly
875 storm-tracks in the western Mediterranean. Quat. Sci. Rev. 197, 352-367.

876 Bartolomei, G., Broglio, A., Cattani, L., Cremaschi, M., Lanzinger, M., Leonardi, P.,1987-
877 88. Nuove ricerche nel deposito pleistocenico della Grotta di Paina sui Colli Berici
878 (Vicenza). Atti Istituto Veneto SS.LL.AA. CXLVI, 112-160.

879 Bar-Matthews, M., Ayalon, A., Kaufman, A., Wasserburg, G.J., 1999. The Eastern
880 Mediterranean paleoclimate as a reflection of regional events: Soreq cave, Israel. Earth
881 and Planetary Science Letters, 166 (1-2), 85-95.

882 Bar-Matthews, M., Avalon, A., Kaufman, A., 2000. Timing and hydrological conditions of
883 sapropel events in the Eastern Mediterranean as evident from speleothems, Soreq cave,
884 Israel. Chemical Geology, 169 (1-2), 145-156.

885 Bavec, M., Verbič, T., 2011. Glacial history of Slovenia. Dev. Quat. Sci. 15, 385–392.

886 Beaulieu, J.-L. de, Reille, M., 1984. A long upper Pleistocene pollen record from Les
887 Echets, near Lyon. Boreas, 1, 111-132.

888 Beaulieu, J.-L. de, Reille, M., 1992a. The last climatic cycle at La Grand Pile (Vosges,
889 France). A new pollen profile. Quaternary Science Reviews, 11, 431–438.

890 Beaulieu, J.-L. de, Reille, M., 1992b. Long Pleistocene sequences from the Velay plateau
891 (Massif Central, France). I. Ribains maar. Vegetation History and Archaeobotany, 1, 233–
892 242.

893 Becker, D., Verheul, J., Zickel, M., Willmes, C., 2015. LGM paleoenvironment of Europe –
894 Map. CRC806-Database, DOI: http://dx.doi.org/10.5880/SFB806.15.

895 Been, E., Hovers, E., Ekshtain, R., Malinsky-Buller, A., Agha, N., Barash, A., Bar-Yosef
896 Mayer, D.E., Benazzi S., Hublin, J-J., Levin, L., Greenbaum N., Mitki, N., Oxilia G., Porat,
897 N., Roskin, J., Soudack, M., Yeshurun, R., Shahack-Gross, R., Nir, N., Stahlschmidt, M.C.,
898 Rak, Y., Barzilai, O., 2017. The first Neanderthal remains from an open-air Middle
899 Palaeolithic site in the Levant. Scientific Reports, 7, 2958.

900 Benazzi, S, Douka, K, Fornai, C, Bauer, C. C., Kullmer, O, Svoboda, J, Pap, I., Mallegni,
901 F., Bayle, P., Coquerelle, M., Condemi, S., Ronchitelli, A., Harvati, K., Weber, G. W., 2011.
902 Early dispersal of modern humans in Europe and implications for Neanderthal behaviour.
903 Nature 479, 525–528.

904 Benazzi, S., Slon, S., Talamo, S., Negrino, F., Peresani, M., Bailey, S.E., Sawyer, S.,
905 Panetta, D., Vicino, G., Starnini, E., Mannino, M.A., Salvadori, P.A., Meyer, M., Pääbo, S.,
906 Hublin, J-J., 2015. The Makers of the Protoaurignacian and Implications for Neandertal
907 Extinction. Science 348, 793-6.

908 Benini, A., Boscato, P., Gambassini, P., 1997. Grotta della Cala (Salerno): industrie litiche
909 e faune uluzziane e aurignaziane. Rivista di Scienze Preistoriche 48, 37–95.

910 Bird, M.I., Ayliffe, L.K., Fifield, L.K., Turney, C.S.M., Cresswell, R.G., Barrows, T.T., David,
911 B., 1999. Radiocarbon dating of “old” charcoal using a wet oxidation, stepped-combustion
912 procedure. Radiocarbon, 41 (2), 127-140.

913 Bird, M.I., Levchenko, V., Ascough, P.L., Meredith, W., Wurster, C.M., Williams, A.,
914 Tilston, E.L., Snape, C.E., Apperley, D.C., 2014. The efficiency of charcoal

915 decontamination for radiocarbon dating by three pre-treatments–ABOX, ABA and
916 hypy. Quaternary Geochronology, 22, 25-32.

917 Blockley, S.P.E., Lane, C.S., Hardiman, M., Rasmussen, S.O., Seierstad, I.K., Steffensen,
918 J.P., Svensson, A., Lotter, A.F., Turney, C.S.M., Bronk Ramsey, C., 2012. Synchronisation
919 of palaeoenvironmental records over the last 60,000 years, and an extended INTIMATE
920 event stratigraphy to 48,000 b2k. Quaternary Science Reviews 36, 2-10.

921 Bond, G., Heinrich, H., Broecker, W., Labeyrie, L., McManus, J., Andrews, J., Huon, S.,
922 Jantschik, R., Clasen, S., Simet, C., Tedesco, K., Klas, M., Bonani, G., and Ivy, S., 1992.
923 Evidence for massive discharges of icebergs into the North Atlantic ocean during the last
924 glacial period, Nature, 360, 245–249.

925 Bond, G., Broecher, W., Johnsen, S.J., MacManus, J., Laberie, L., Jouzel, J., Bonani, G.,
926 1993. Correlations between climate records from North Atlantic sediments and Greenland
927 ice, Nature, 365, 143–147.

928 Boretto, G., Zanchetta, G., Ciulli, L., Bini, M., Fallick, E., Lezzerini, M., Colonese A.C.,
929 Zembo, I., Trombino, L., Regattieri, E., Sarti, G., 2017. The loess deposits of Buca Dei
930 Corvi section (Central Italy): Revisited. Catena, 151, 225-237.

931 Borzatti von Löwenstern, E., 1965. La grotta di Uluzzo (campagna di scavi 1964). Rivista
932 di Scienze Preistoriche 19, 41-52.

933 Borzatti von Löwenstern, E., 1966. Alcuni aspetti del Musteriano nel Salento. (La grotta-
934 riparo di Torre dell'Alto e la grotta di Uluzzo C). Scavi 1965 e 1966. Rivista di Scienze
935 Preistoriche 21, 203–287.

936 Borzatti von Löwenstern, E., 1970. Prima campagna di scavi nella grotta "Mario
937 Bernardini" (Nardò - Lecce). Rivista di Scienze Preistoriche 25, 89–125.

938 Broecker, W.S.T., Peng, H., Jouzel, J., Russell, G., 1990. The magnitude of global fresh-
939 water transports of importance to ocean circulation. Climate Dynamics, 4, 73-79.

940 Bruins, H. J., Keller, J., Klügel, A., Kisch, H. J., Katra, I., van der Plicht, J., 2019. Tephra in
941 caves: Distal deposits of the Minoan Santorini eruption and the Campanian super-eruption.
942 Quaternary International, 499, 135-147.

943 Buoncristiani, J.-F., Campy, M. 2004. Palaeogeography of the last two glacial episodes in
944 the Massif Central, France. Dev. Quat. Sci. 2, 111-112.

945 Burjachs, F., López-García, J.M., Allué, E., Blain, H.A., Rivals, F., Bennàsar, M., Expósito,
946 I., 2012. Palaeoecology of Neanderthals during Dansgaard–Oeschger cycles in
947 northeastern Iberia (Abric Romaní): from regional to global scale. Quaternary
948 International, 247, 26-37.

949 Butzin, M., Köhler, P., Lohmann, G., 2017. Marine radiocarbon reservoir age simulations
950 for the past 50,000 years. Geophysical Research Letters, 44 (16), 8473-8480.

951 Cacho, I., Grimalt, J. O., Pelejero, C., Canals, M., Sierro, F. J., Flores, J. A., Shackleton,
952 N., 1999. Dansgaard-Oeschger and Heinrich event imprints in Alboran Sea
953 paleotemperatures. Paleoceanography, 14 (6), 698-705.

954 Carraro F., Sauro U., 1979. Il Glacialismo “locale” Wurmiano del Massiccio del Grappa
955 (Provincie di Treviso e di Vicenza). Geografia Fisica e Dinamica Quaternaria, 2(1), 6-16.

956 Cattani L., Renault-Miskovsky, J., 1983-84. Etude pollinique du remplissage de la Grotte
957 du Broion (Vicenza, Italie). Paléoclimatologie du Würmien en Vénétie. Bullettin Association
958 Française Étude du Quaternaire, XVI (4), 197-212.

959 Cattani, L., 1990. Steppe environments at the margin of the Venetian Pre-Alps during the
960 Pleniglacial and Late-Glacial periods. In: Cremaschi M. (ed), The Loess in Northern and

961 Central Italy: a Loess Basin between the Alps and the Mediterranean Region, Quaderni di
962 Geodinamica Alpina e Quaternaria., 1: 133-137.

963 Cheng, H., Lawrence Edwards, R., Southon, J., Matsumoto, K., Feinberg, J.M., Sinha, A.,
964 Zhou, W., Li, H., Li, X., Xu, Y., Chen, S., Tan, M., Wang, Q., Wang, Y., Ning, Y., 2018.
965 Atmospheric $^{14}C/^{12}C$ changes during the last glacial period from Hulu Cave. Science, 362,
966 1293-1297.

967 Chiesa, S., Coltorti, M., Cremaschi, M., Ferraris, M., Prosperi, l., 1990. Loess sedimenta-
968 tion and quaternary deposits in the Marche province. In Cremaschi, M. (Ed.), The loess in
969 northern and central Italy. A loess basin between the Alps and the Mediterranean region,
970 Quaderni di Geodinamica Alpina e Quaternaria 1, Milano, 103-130.

971 Combourieu-Nebout, N., Turon, J.-L., Zahn, R., Capotondi, L., Londeix, L., Pahnke, K.,
972 2002. Enhanced aridity and atmospheric high-pressure stability over the western
973 Mediterranean during the North Atlantic cold events of the past 50 k.y. Geology 30, 863–
974 866.

975 Combourieu-Nebout, N., Peyron, O., Dormoy, I., Desprat, S., Beaudouin, C., Kotthoff, U.,
976 Marret, F., 2009. Rapid climatic variability in the west Mediterranean during the last 25 000
977 years from high resolution pollen data. Climate of the Past, 5 (3), 503-521.

978 Copeland, L., Yazbeck, C., 2002. Inventory of Stone Age Sites in Lebanon. In: New and
979 Revised, Part III, vol. 55. Melanges de l'Universite Saint-Joseph, 121-325.

980 Costa, A., Folch, A., Macedonio, G., Giaccio, B., Isaia, R., Smith, V.C., 2012. Quantifying
981 volcanic ash dispersal and impact of the Campanian Ignimbrite super-eruption.
982 Geophysical Research Letters, 39 (10).

983 Cremaschi, M., 1990. The loess in northern and central Italy. A loess basin between the
984 Alps and the Mediterranean region. Quaderni di Geodinamica Alpina e Quaternaria 1,
985 Milano, Italy.

Cremaschi, M., 2004. Late Pleistocene loess. In: Antonioli, F., Vai, G.B. (Eds.), Litho-palaeoenvironmental Maps of Italy During the Last Two Climatic Extremes. Climex Maps Italy e Explanatory Notes. Bologna, 34–37.

Cremaschi, M., Zerboni, A., Nicosia, C., Negrino, F., Rodnight, H., Spötl, C., 2015. Age, soil-forming processes, and archaeology of the loess deposits at the Apennine margin of the Po Plain (northern Italy). New insights from the Ghiardo area. Quaternary International, 376, 173–188.

Cremonesi, G., 1987. Due complessi d'arte del Paleolitico superiore: la Grotta Polesini e la Grotta delle Veneri. Atti del VI Convegno di Preistoria e Protostoria. Storia della Daunia, 2, 35-50.

Crouvi, O., Amit, R., Enzel, Y., Gillespie, A.R., 2010. The role of active sand seas in the formation of desert loess. Quaternary Science Reviews, 29, 2087–2098.

Daniau, A. L., Sánchez-Goñi, M. F., Beaufort, L., Laggoun-Défarge, F., Loutre, M. F., Duprat, J., 2007. Dansgaard–Oeschger climatic variability revealed by fire emissions in southwestern Iberia. Quaternary Science Reviews, 26(9-10), 1369-1383.

Daniau, A. L., Goñi, M.F.S., Duprat, J., 2009. Last glacial fire regime variability in western France inferred from microcharcoal preserved in core MD04-2845, Bay of Biscay. Quaternary Research, 71(3), 385-396.

Dansgaard, W., Johnsen, S.J., Clausen, H.B., Dahl-Jensen, D., Gundestrup, N.S., Hammer, C.U., Hvidberg, C.S., Steffensen, J.P., Sveinbjorndottir, A.E., Jouzel, J., Bond, G., 1993. Evidence for general instability of past climate from a 250-kyr ice-core record. Nature, 364, 218-220.

Darfeuil, S., Ménot, G., Giraud, X., Rostek, F., Tachikawa, K., Garcia, M., Bard, É., 2016. Sea surface temperature reconstructions over the last 70 kyr off Portugal: Biomarker data and regional modeling. Paleoceanography, 31 (1), 40-65.

1011 Darlas, A., Psathi, E., 2016. The Middle and Upper Paleolithic on the western coast of the
1012 Mani Peninsula (southern Greece). In Paleoanthropology of the Balkans and Anatolia (pp.
1013 95-117). Springer, Dordrecht.

1014 de Goër, H. 1972. La Planèze de Saint Flour: formes et dépots glaciaires. Annales de la
1015 faculté des Sciences de Clermont-Ferrand, 48, 1-204.

1016 Delmas, M., 2015. The Last Maximum Ice Extent and subsequent deglaciation of the
1017 Pyrenees: an overview of recent research. Cuadernos de Investigación Geográfica, 41,
1018 359-387.

1019 Delpiano, D., Peresani, M., Bertola, S., Cremaschi, M., Zerboni, A., 2019. Lashed by the
1020 wind: short-term Middle Palaeolithic occupations within the loess-palaeosoil sequence at
1021 Monte Netto (Northern Italy). Quaternary International, 502, 137-147.

1022 Dini, M., Tozzi, C., 2012. La Transizione Paleolitico Medio-Paleolitico Superiore nella
1023 Grotta La Fabbrica (Grosseto-Toscana). Atti della Società Toscana di Scienze Naturali -
1024 Memorie Serie A, 117-119.

1025 Douka, K., Higham, T. F., Wood, R., Boscato, P., Gambassini, P., Karkanas, P., Peresani,
1026 M., Ronchitelli, A. M., 2014. On the chronology of the Uluzzian. Journal of Human
1027 Evolution, 68, 1-13.

1028 Douka, K., Grimaldi, S., Boschian, G., del Lucchese, A., Higham, T. F., 2012. A new
1029 chronostratigraphic framework for the Upper Palaeolithic of Riparo Mochi (Italy). Journal of
1030 Human Evolution, 62 (2), 286-299.

1031 Douka, K., Bergman, C.A., Hedges, R.E.M., Wesselingh, F.P., Higham, T., 2013.
1032 Chronology of Ksar Akil (Lebanon) and implications for the colonization of Europe by
1033 anatomically modern humans. PLoS ONE, 8, e72931.

1034 Douka, K., Higham, T., 2017. The chronological factor in understanding the Middle and
1035 Upper Paleolithic of Eurasia. Current Anthropology, 58 (S17), S480-S490.

1036 Drescher-Schneider, R., Jacquat, C., Schoch, W., 2007. Palaeobotanical investigations at
1037 the mammoth site of Niederweningen (Kanton Zürich). Switzerland. Quaternary
1038 International, 164-165, 113-129.

1039 Ehlers, J., Gibbard, P.L., Hughes, P.D., 2011. Quaternary Glaciations e Extent and
1040 Chronology, vol. 15. Elsevier, Amsterdam, 1126.

1041 Engel, Z., Mentlík, P., Braucher, R., Minár, J., Léanni, L., Aster Team, 2015.
1042 Geomorphological evidence and ^{10}Be exposure ages for the last glacial maximum and
1043 deglaciation of the Velká and Malá Studená dolina valleys in the high Tatra mountains,
1044 central Europe. Quaternary Science Reviews 124, 106-123.

1045 European Environment Agency, 2015. European ecosystem assessment - concept, data,
1046 and implementation. Contribution to Target 2 Action 5 Mapping and Assessment of
1047 Ecosystems and their Services (MAES) of the EU Biodiversity Strategy to 2020. Technical
1048 Report 06/2015.

1049 Falcucci, A., Conard, N.J., Peresani, M., 2017. A critical assessment of the
1050 Protoaurignacian lithic technology at Fumane Cave and its implications for the definition of
1051 the earliest Aurignacian. PloS ONE, 12 (12), e0189241.

1052 Falcucci, A., Peresani, M., 2018. Protoaurignacian core reduction procedures: blade and
1053 bladelet technologies at Fumane Cave. Lithic Technology, 43(2), 125-140.

1054 Farquhar, G.D., 1997. Carbon dioxide and vegetation, Science, 278 (5342), 1411.

1055 Fedele, F.G., Giaccio, B., Isaia, R., Orsi, G., 2003. The Campanian Ignimbrite eruption,
1056 Heinrich Event 4, and the Paleolithic change in Europe: a high-resolution investigation.

1057 Volcanism and Earth's Atmosphere, eds Robock A., Oppenheimer C. (AGU Geophys,
1058 Washington, DC), 301–325.

1059 Fedele, F.G., Giaccio, B., Hajdas, I., 2008. Timescales and cultural process at 40,000 BP
1060 in the light of the Campanian Ignimbrite eruption, western Eurasia. Journal of Human
1061 Evolution, 55, 834–857.

1062 Ferraro, F., 2009. Age, sedimentation, and soil formation in the Val Sorda loess sequence,
1063 Northern Italy. Quaternary International, 204, 54–64.

1064 Fischer, H., Fundel, F., Ruth, U., Twarloh, B., Wegner, A., Udisti, R., Becagli, S.,
1065 Castellano, E., Morganti, A., Severi, M., Wolff, E., Littot G., Röthlisberger, R., Mulvaney,
1066 R., Hutterli, M. A., Kaufmann, P., Federer, U., Lambert, F., Bigler M., Hansson, M., Jonsell,
1067 U., de Angelis, M., Boutron, C., Siggaard-Andersen, M.-L., Steffensen, J. P., Barbante, C.,
1068 Gaspari, V., Gabrielli, P., Wagenbach, D., 2007a. Reconstruction of millennial changes in
1069 dust emission, transport and regional sea ice coverage using the deep EPICA ice cores
1070 from the Atlantic and Indian Ocean sector of Antarctica. Earth and Planetary Science
1071 Letters, 260 (1), 340-354.

1072 Fischer, H., Siggaard-Andersen, M.L., Ruth, U., Röthlisberger, R., Wolff, E., 2007b.
1073 Glacial/interglacial changes in mineral dust and sea-salt records in polar ice cores:
1074 Sources, transport, and deposition. Reviews of Geophysics, 45 (1).

1075 Fleitmann, D., Cheng, H., Badertscher, S., Edwards, R.L., Mudelsee, M., Göktürk, O.M.,
1076 Fankhauser A., Pickering R., Raible C.C., Matter A, Kramers J, Tüysüz O., 2009. Timing
1077 and climatic impact of Greenland interstadials recorded in stalagmites from northern
1078 Turkey. Geophysical Research Letters, 36 (19).

1079 Fletcher, W.J., Sánchez Goñi, M.F., 2008. Orbital-and sub-orbital-scale climate impacts on
1080 vegetation of the western Mediterranean basin over the last 48,000 yr. Quaternary
1081 Research, 70 (3), 451-464.

1082 Fletcher, W.J., Sánchez Goñi, M.F., Peyron, O., Dormoy, I., 2010a. Abrupt climate
1083 changes of the last deglaciation detected in a Western Mediterranean forest record.
1084 Climate of the Past, 6, 245-264.

1085 Fletcher, W.J., Sánchez Goñi, M. F., Allen, J. R. M., Cheddadi, R., Comborieu-Nebout, N.,
1086 Huntley, B., Lawson, I., Londeix, L., Magri, D., Margari, V., Müller, U. C., Naughton, F.,
1087 Novenko, E., Roucoux, K., Tzedakis, P.C., 2010b. Millennial scale variability during the
1088 last glacial in vegetation records from Europe. Quaternary Science Reviews. Quaternary
1089 Science Reviews, 29 (21-22), 2839-2864.

1090 Floss, H., 2003. Did they meet or not? Observations on Châtelperronian and Aurignacian
1091 settlement patterns in eastern France. In (Zilhao & Errico, eds): The chronology of the
1092 Aurignacian and of the transitional technocomplexes. Dating, stratigraphies, cultural
1093 implications. Actes 14e Congrès UISPP, Université de Liège, Belgique, 2-8 sept. 2001.
1094 Trabalhos de Arqueologia n° 33, 273-287.

1095 Flückiger, J., Knutti, R., White, J.W., 2006. Oceanic processes as potential trigger and
1096 amplifying mechanisms for Heinrich events. Paleoceanography, 21 (2).

1097 Follieri, M., Magri, D., Sadori, L., 1988. 250,000-year pollen record from Valle di
1098 Castiglione (Roma). Pollen et Spores 30, 329-356.

1099 Follieri, M., Giardini, M., Magri, D., Sadori, L., 1998. Palynostratigraphy of the last glacial
1100 period in the volcanic region of central Italy. Quaternary International, 47, 3-20.

1101 Fontana, A., Mozzi, P., Marchetti, M., 2014. Alluvial fans and megafans along the southern
1102 side of the Alps. Sediment. Geol. 301, 150–171.

1103 Forno, M.G., Gianotti, F., Racca, G. 2010. Significato paleoclimatico dei rapporti tra il
1104 glacialismo principale e quello tributario nella bassa Valle della Dora Baltea. Il Quaternario
1105 23, 105-124.

1106 Franciscus, R.G., 1999. Neandertal nasal structures and upper respiratory tract
1107 “specialization”. Proceedings of the National Academy of Sciences, 96 (4), 1805-1809.

1108 Frechen, M., Horváth, E., Gábris, G., 1997. Geochronology of Middle and Upper
1109 Pleistocene loess sections in Hungary. Quaternary Research, 48, 291–312.

1110 Furlanetto, G., Ravazzi, C., Badino, F., Brunetti, M., Champvillair, E., Maggi, V., 2019.
1111 Elevational transects of modern pollen samples: Site-specific temperatures as a tool for
1112 palaeoclimate reconstructions in the Alps. The Holocene, 29(2), 271-286.

1113 Gambassini, P., 1997. Il Paleolitico di Castelcivita: culture e ambiente. Electa, Napoli, Italy.

1114 Genty, D., Blamart, D., Ouahdi, R., Gilmour, M., Baker, A., Jouzel, J., Van-Exter, S., 2003.
1115 Precise dating of Dansgaard–Oeschger climate oscillations in western Europe from
1116 stalagmite data. Nature, 421 (6925), 833.

1117 Genty, D., Blamart, D., Ghaleb, B., Plagnes, V., Causse, C., Bakalowicz, M., Zouari, K.,
1118 Chkir N., Hellstrom, J., Wainer, K., Bourges, F., 2006. Timing and dynamics of the last
1119 deglaciation from European and North African $\delta^{13}C$ stalagmite profiles—comparison with
1120 Chinese and South Hemisphere stalagmites. Quaternary Science Reviews, 25 (17-18),
1121 2118-2142.

1122 Genty, D., Combourieu-Nebout, N., Peyron, O., Blamart, D., Wainer, K., Mansuri, F.,
1123 Ghaleb, B., Isabello, L., Dormoy, I., von Grafenstein, U., Bonelli, S., Landais A., Brauer, A.,
1124 2010. Isotopic characterization of rapid climatic events during OIS3 and OIS4 in Villars
1125 Cave stalagmites (SW-France) and correlation with Atlantic and Mediterranean pollen
1126 records. Quaternary Science Reviews, 29 (19), 2799-2820.

1127 Giaccio, B., Hajdas, I., Peresani, M., Fedele, F.G., Isaia, R., 2006. The Campanian
1128 Ignimbrite tephra and its relevance for the timing of the Middle to Upper Palaeolithic shift.
1129 When Neanderthals and Modern Humans Met, ed Conard N.J. (Kerns Verlag, Tübingen,
1130 Germany), 343–375.

1131 Giaccio, B., Isaia, R., Fedele, F.G., Di Canzio, E., Hoffecker, J., Ronchitelli, A., Sinitsyn,
1132 A.A., Anikovich, M., Lisitsyn S.N., Popov, V.V. 2008. The Campanian Ignimbrite and
1133 Codola tephra layers: Two temporal/stratigraphic markers for the Early Upper Palaeolithic
1134 in southern Italy and eastern Europe. Journal of Volcanology and Geothermal Research,
1135 177, 208–226.

1136 Gianotti, F., Forno, M.G., Ivy-Ochs S., Monegato, G., Pini, R., Ravazzi, C., 2015.
1137 Stratigraphy of the Ivrea morainic amphitheatre (NW Italy): an updated synthesis. Alpine
1138 and Mediterranean Quaternary, 28, 29-58.

1139 Giaccio, B., Hajdas, I., Isaia, R., Deino, A., Nomade, S., 2017. High-precision ^{14}C and
1140 $^{40}Ar/^{39}Ar$ dating of the Campanian Ignimbrite (Y-5) reconciles the time-scales of climatic-
1141 cultural processes at 40 ka. Scientific reports, 7, 45940.

1142 Giraudi, C., Giaccio, B., 2016. Middle Pleistocene glaciations in the Apennines, Italy: new
1143 chronological data and preservation of the glacial record. In: Hughes, P.D. & Woodward,
1144 J.C. (eds) Quaternary Glaciation in the Mediterranean Mountains. Geological Society,
1145 London, Special Publications, 433, 161-178.

1146 Govin, A., Capron, E., Tzedakis, P.C., Verheyden, S., Ghaleb, B., Hillaire-Marcel, C., St-
1147 Onge, G., Stoner, J.S., Bassinot, F., Bazin, L., Blunier, T., Combourieu-Nebout, N., El
1148 Ouahabi, A., Genty, D., Gersonde, R., Jimenez-Amat, P., Landais, A., Martrat, B.,
1149 Masson-Delmotte, V., Parrenin, F., Seidenkrantz, M.-S., Veres, D., Waelbroeck, C., Zahn,
1150 R., 2015. Sequence of events from the onset to the demise of the Last Interglacial:
1151 Evaluating strengths and limitations of chronologies used in climatic archives. Quaternary
1152 Science Reviews, 129, 1-36.

1153 Grant, K.M., Rohling, E.J., Bar-Matthews, M., Ayalon, A., Medina-Elizalde, M., Ramsey, C.
1154 B., Satow, C., Roberts, A.P., 2012. Rapid coupling between ice volume and polar
1155 temperature over the past 150,000 years. Nature, 491 (7426), 744.

1156 Greenbaum, G., Friesem, D. E., Hovers, E., Feldman, M. W., Kolodny, O., 2018. Was
1157 inter-population connectivity of Neanderthals and modern humans the driver of the Upper
1158 Paleolithic transition rather than its product?. Quaternary Science Reviews.

1159 Gromig, R., Mechernich, S., Ribolini, A., Wagner, B., Zanchetta, G., Isola, I., Bini, M.,
1160 Dunai, T., 2018. Evidence for a Younger Dryas deglaciation in the Galicica Mountains
1161 (FYROM) from cosmogenic ^{36}Cl. Quaternary International, 464, 352–363.

1162 Guillevic, M., Bazin, L., Landais, A., Stowasser, C., Masson-Delmotte, V., Blunier, T.,
1163 Eynaud, F., Falourd, S., Michel, E., Minster, B., Popp, T., Prié, F., Vinther, B. M., 2014.
1164 Evidence for a three-phase sequence during Heinrich Stadial 4 using a multiproxy
1165 approach based on Greenland ice core records. Climate of the Past, 10 (6), 2115-2133.

1166 Guiot, J., Reille, M., Beaulieu, J.L. de, Pons, A., 1992. Calibration of the climatic signal in a
1167 new pollen sequence from La Grande Pile. Climate Dynamics, 6 (3-4), 259-264.

1168 Güleç, E., Kuhn, S.L., Stiner, M. C., 2002. The early Upper Palaeolithic of Üçağızlı Cave,
1169 Turkey. Antiquity, 76 (293), 615-616.

1170 Haase, D., Fink, J., Haase, G., Ruske, R., Pécsi, M., Richter, H., Altermann, M., Jäger, K.
1171 D., 2007. Loess in Europe - its spatial distribution based on a European Loess Map, scale
1172 1: 2,500,000. Quaternary Science Reviews, 26 (9-10), 1301-1312.

1173 Haesaerts, P., Borziac, I., Chekha, V.P., Chirica, V., Damblon, F., Drozdov, N.I., Orlova,
1174 L.A., Pirson, S., van der Plicht, J., 2009. Climatic signature and radiocarbon chronology of
1175 middle and late pleniglacial loess from Eurasia: comparison with the marine and
1176 Greenland records. Radiocarbon, 51 (1), 301-318.

1177 Harrison, S.P., Sánchez Goñi, M.F., 2010. Global patterns of vegetation response to
1178 millennial-scale variability and rapid climate change during the last glacial
1179 period. Quaternary Science Reviews, 29 (21-22), 2957-2980.

1180 Heinrich, H., 1988. Origin and consequences of cyclic ice rafting in the northeast Atlantic
1181 Ocean during the past 130,000 years. Quaternary research, 29 (2), 142-152.

1182 Heiri, O., Koinig, K.A., Spötl, C., Barrett, S., Brauer, A., Drescher-Schneider, R.,G. Dorian,
1183 Ivy-Ochs, S., Kerschner, H., Luetscher, M., Moran, A., Nicolussi, K., Preusser, F.,
1184 Schmidt, R., Schoeneich, P., Schwörer, C., Sprafke, T., Terhorst, B., Tinner, W., 2014.
1185 Palaeoclimate records 60–8 ka in the Austrian and Swiss Alps and their
1186 forelands. Quaternary Science Reviews, 106, 186-205.

1187 Hemming, S.R., 2004. Heinrich events: Massive late Pleistocene detritus layers of the
1188 North Atlantic and their global climate imprint. Reviews of Geophysics, 42 (1), RG1005,
1189 doi:10.1029/2003RG000128.

1190 Hershkovitz, I., Marder, O., Ayalon, A., Bar-Matthews, M., Yasur, G., Boaretto, E.,
1191 Caracuta V., Alex, B., Frumkin, A., Goder-Goldberger, M., Gunz, P., Holloway, R.L.,
1192 Latimer, B., Lavi, R., Matthews, A., Slon, Vi., Bar-Yosef Mayer, D., Berna, F., Bar-Oz, G.,
1193 Yeshurun, R., May, H., Hans, M.G., Weber, G.W., Barzilai, O., 2015. Levantine cranium
1194 from Manot Cave (Israel) foreshadows the first European modern humans. Nature, 520
1195 (7546), 216.

1196 Higham, T., Brock, F., Peresani, M., Broglio, A., Wood, R., Douka, K., 2009. Problems with
1197 radiocarbon dating the Middle to Upper Palaeolithic transition in Italy. Quaternary Science
1198 Reviews, 28 (13-14), 1257-1267.

1199 Higham, T., 2011. European Middle and Upper Palaeolithic radiocarbon dates are often
1200 older than they look: problems with previous dates and some remedies. Antiquity, 85
1201 (327), 235-249.

1202 Higham, T., Douka, K., Wood, R., Ramsey, C.B., Brock, F., Basell, L., Camps, M.,
1203 Arrizabalaga, A., Baena, J., Barroso-Ruiz, C., Bergman, C., Boitard, C., Boscato, P.,
1204 Caparros, M., Conard, N. J., Draily, C., Froment, A., Galvan, B., Gambassini, P., Garcia-
1205 Moreno, A., Grimaldi, S., Haesaerts, P., Holt, B., Iriarte-Chiapusso, M. J., Jelinek, A.,

1206 Jorda Pardo, J.F., Maillo-Fernandez, J.M., Marom, A., Maroto J, Menendez M, Metz L,
1207 Morin E, Moroni, A., Negrino, F., Panagopoulou, E., Peresani, M., Pirson, S., de la Rasilla,
1208 M., Riel-Salvatore, J., Ronchitelli, A., Santamaria, D., Semal, P., Slimak, L., Soler, J.,
1209 Soler, N., Villaluenga, A., Pinhasi, R., Jacobi, R., 2014. The timing and spatiotemporal
1210 patterning of Neanderthal disappearance. Nature 512, 306-309.

1211 Hoffecker, J.F., Holliday, V.T., Anikovich, M. V., Sinitsyn, A.A., Popov, V.V., Lisitsyn, S.N.,
1212 Levkovskaya, G.M., Pospelova, G.A., Forman, S.L., Giaccio, B., 2008. From the bay of
1213 Naples to the River Don: The Campanian Ignimbrite eruption and the Middle to Upper
1214 Paleolithic transition in eastern Europe. Journal of Human Evolution, 55, 858–70.

1215 Hoffecker, J.F., 2009. The spread of modern humans in Europe. Proceedings of the
1216 National Academy of Sciences, 106 (38), 16040-16045.

1217 Holtmeier, F. K.,1985. Climatic stress influencing the physiognomy of trees at the polar
1218 and mountain timberline. Eidgenössische Anstalt für das Forstliche Versuchswesen,
1219 Berichte 270, 31–40.

1220 Holtmeier, F. K., 2009. Mountain timberlines: ecology, patchiness, and dynamics (Vol. 36).
1221 Springer Science & Business Media.

1222 Hublin, J.-J., 2014. The modern human colonization of western Eurasia: when and where?
1223 Quaternary Science Reviews, 1–17.

1224 Hublin, J-J., 2015. The Modern Human Colonization of Western Eurasia: When and
1225 Where? Quaternary Science Reviews, 18, 194–210.

1226 Hughes, A.L.C., Gyllencreutz, R., Lohne, Ø.S., Mangerud, J., Svendsen, J.I., 2016. The
1227 last Eurasian ice sheets - a chronological database and time-slice reconstruction, DATED-
1228 1. Boreas, 45, 1-45.

1229 Hughes, P.D., Woodward, J.C., 2016. Quaternary glaciation in the Mediterranean
1230 mountains: a new synthesis. In: Hughes, P.D. & Woodward, J.C. (eds) Quaternary
1231 Glaciation in the Mediterranean Mountains. Geological Society, London, Special
1232 Publications, 433, pp. 1-23. doi.org/10.1144/SP433.14

1233 Hussain, S. T., Floss, H., 2016. Streams as entanglement of nature and culture: European
1234 Upper Paleolithic river systems and their role as features of spatial organization. Journal of
1235 archaeological method and theory, 23(4), 1162-1218.

1236 Iglesias, V., Yospin, G.I., Whitlock, C., 2015. Reconstruction of fire regimes through
1237 integrated paleoecological proxy data and ecological modeling. Frontiers in plant
1238 science, 5, 785.

1239 Ivy-Ochs, S., Kerschner, H., Reuther, A., Preusser, F., Heine, K., Maisch, M., Kubik, P.W.,
1240 Schlüchter, C., 2008. Chronology of the last glacial cycle in the European Alps. Journal of
1241 Quaternary Science 23, 559–573.

1242 Ivy-Ochs, S., Lucchesi, S., Baggio, P., Fioraso, G., Gianotti, G., Monegato, G., Graf, A.A.,
1243 Akscar, N., Christl, M., Carraro, F., Forno, M.G., Schlüchter, C., 2018. New
1244 geomorphological and chronological constraints for glacial deposits in the Rivoli-Avigliana
1245 end-moraine system and the lower Susa Valley (Western Alps, NW Italy). Journal of
1246 Quaternary Science 33, 550–562.

1247 Jobbagy, E.G., Jackson, R.B., 2000. Global controls of forest line elevation in the northern
1248 and southern hemispheres. Global Ecology and Biogeography, 9 (3), 253-268.

1249 Jorda, M., Rosique, T., Evin, J., 2000. Données nouvelles sur l'age du dernier maximum
1250 glaciaire dans les Alpes méridionales françaises. Comptes Rendus de l'Académie des
1251 Sciences - Series IIA - Earth and Planetary Science 331, 187–193.

1252 Kelly, M.A., Kubik, P.W., Von Blanckenburg, F., Schlüchter, C., 2004. Surface exposure
1253 dating of the Great Aletsch Glacier Egesen moraine system, western Swiss Alps, using the
1254 cosmogenic nuclide 10Be. Journal of Quaternary Science, 19 (5), 431-441.

1255 Kindler, P., Guillevic, M., Baumgartner, M., Schwander, J., Landais, A., Leuenberger, M.,
1256 2014. Temperature reconstruction from 10 to 120 kyr b2k from the NGRIP ice core.
1257 Climate of the Past, 10 (2), 887-902.

1258 Körner, C., Paulsen, J., 2004. A world-wide study of high-altitude treeline temperatures. J.
1259 Biogeogr. 31 (5), 713-732.

1260 Kuhlemann, J., Rohling, E.J., Krumrei, I., Kubik, P., Ivy-Ochs, S., Kucera, M., 2008.
1261 Regional Synthesis of Mediterranean atmospheric circulation during the Last Glacial
1262 Maximum. Science, 321(5894), 1338-1340.

1263 Kuhlemann, J., Milivojevic, M., Krumrei, I., Kubik, P.W., 2009. Last glaciation of the Sara
1264 Range (Balkan Peninsula): increasing dryness from the LGM to the Holocene. Austrian
1265 Journal of Earth Sciences, 102, 146–158.

1266 Kuhn, S.L., Stiner, M.C., Güleç, E., Özer, I., Yilmaz, H., Baykara, I., Açikkol, A., Goldberg,
1267 P., Molina, K.M., Ünay, E., Suata-Alpaslan, F., 2009. The early Upper Paleolithic
1268 occupations at Üçağızlı Cave (Hatay, Turkey). Journal of Human Evolution, 56 (2), 87-113.

1269 Kukla, G.J., 1975. Loess stratigraphy of Central Europe. In: Butzer, K.W., Isaac, L.I.
1270 (Eds.), After the Australopithecines. Mouton Publishers, The Hague, 99–187.

1271 Lambeck, K., Purcell, A., Zhao, J., Svensson, N.-O., 2010. The Scandinavian Ice Sheet:
1272 from MIS 4 to the end of the Last Glacial Maximum. Boreas, 39, 410-435.

1273 Lambeck, K., Rouby, H., Purcell, A., Sun, Y., Sambridge, M., 2014. Sea level and global
1274 ice volumes from the Last Glacial Maximum to the Holocene. PNAS, 111(43), 15296-
1275 15303.

1276 Lehmkuhl, F., Bösken, J., Hošek, J., Sprafke, T., Marković, S.B., Obreht, I., Hambach, U.,
1277 Sümegi, P., Thiemann, A., Steffens, S., Lindner, H., Veres, D., Zeeden, C., 2018a. Loess
1278 distribution and related Quaternary sediments in the Carpathian Basin. Journal of Maps,
1279 14, 673–682.

1280 Lehmkuhl, F., Pötter, S., Pauligk, A., Bösken, J., 2018b. Loess and other Quaternary
1281 sediments in Germany. Journal of Maps, 14, 330–340.

1282 Leonardi, P., Broglio, A., 1966. Datazione assoluta di un'industria musteriana della grotta
1283 del Broion. Rivista di Scienze Preistoriche 21, (2), 397-405.

1284 Leroy, S.A.G., Giralt, S., Francus, P., Seret, G., 1996. The high sensitivity of the
1285 palynological record in the Vico maar lacustrine sequence (Latium, Italy) highlights the
1286 climatic gradient through Europe for the last 90 ka. Quaternary Science Reviews, 15 (2-3),
1287 189-201.

1288 Lézine, A. M., Von Grafenstein, U., Andersen, N., Belmecheri, S., Bordon, A., Caron, B.,
1289 Cazet, J.-P., Erlenkeuser, H., Fouache, E., Grenier, C., Huntsman-Mapila, P., Hureau-
1290 Mazaudier, D., Manelli, D., Mazaud, A., Robert C., Sulpizio, R., Tiercelin, J.-J., Zanchetta,
1291 G., Zeqollari, Z., 2010. Lake Ohrid, Albania, provides an exceptional multi-proxy record of
1292 environmental changes during the last glacial–interglacial cycle. Palaeogeography,
1293 Palaeoclimatology, Palaeoecology, 287 (1-4), 116-127.

1294 Lindner, H., Lehmkuhl, F., Zeeden, C., 2017. Spatial loess distribution in the eastern
1295 Carpathian Basin: a novel approach based on geoscientific maps and data. Journal of
1296 Maps, 13, 173–181.

1297 Lisiecki, L.E., Raymo, M.E., 2005. A Pliocene-Pleistocene stack of 57 globally distributed
1298 benthic $\delta^{18}O$ records. Paleoceanography, 20 (1).

1299 Lowe, J., Barton, N., Blockley, S., Ramsey, C.B., Cullen, V.L., Davies, W., Gamble, C.,
1300 Grant, K., Hardiman, M., Housley, R., Lane, C.S., Lee, S., Lewis, M., MacLeod, A.,

1301 Menzies, M., Müller, W., Pollard, M., Price, C., Roberts A.P., Rohling, E.J., Satow, C.,
1302 Smith, V.C., Stringer, C.B., Tomlinson, E.L., White, D., Albert, P., Arienzo, I., Barker, G.,
1303 Borić, D., Carandente, A., Civetta, L., Ferrier, C., Guadelli, J.-L., Karkanas, P.,
1304 Koumouzelis, M., Müller, U.C., Orsi, G., Pross, J., Rosi, M., Shalamanov-Korobar, L.,
1305 Sirakov, N, Tzedakis, P.C., 2012. Volcanic ash layers illuminate the resilience of
1306 Neanderthals and early modern humans to natural hazards. Proceedings of the National
1307 Academy of Sciences, 109, 13532–13537.

1308 Magri, D., 1994. Late-Quaternary changes of plant biomass as recorded by pollen-
1309 stratigraphical data: a discussion of the problem at Valle di Castiglione, Italy. Review of
1310 Palaeobotany and Palynology, 81 (2-4), 313-325.

1311 Magri, D., 2008. Two long micro-charcoal records from central Italy. Proceedings of the
1312 Third International Meeting of Anthracology, BAR International Series, 1807, 167-175.

1313 Magri, D., Sadori, L., 1999. Late Pleistocene and Holocene pollen stratigraphy at Lago di
1314 Vico, central Italy. Vegetation History and Archaeobotany, 8 (4), 247-260.

1315 Magri, D., 1999. Late Quaternary vegetation history at Lagaccione near Lago di Bolsena
1316 (central Italy). Review of Palaeobotany and Palynology, 106 (3-4), 171-208.

1317 Makos, M., Rinterknecht, V., Braucher, R., Toloczko-Pasek, A., ASTER Team, 2018. Last
1318 Glacial Maximum and Lateglacial in the Polish High Tatra Mountains - Revised
1319 deglaciation chronology based on the ^{10}Be exposure age dating. Quat. Sc. Rev. 187, 130-
1320 156.

1321 Mangerud, J., Gulliksen, S., Larsen, E., 2010. ^{14}C-dated fluctuations of the western flank of
1322 the Scandinavian Ice Sheet 45–25 kyr BP compared with Bølling–Younger Dryas
1323 fluctuations and Dansgaard–Oeschger events in Greenland. Boreas, 39 (2), 328-342.

1324 Marcott, S.A., Clark, P. U., Padman, L., Klinkhammer, G.P., Springer, S. R., Liu, Z., Otto-
1325 Bliesner, B. L., Carlson, A. E., Ungerer, A., Padman, J., He, F., Cheng J., Schmittner, A.,

2011. Ice-shelf collapse from subsurface warming as a trigger for Heinrich events. Proceedings of the National Academy of Sciences, 108 (33), 13415-13419.

Marciani, G, Ronchitelli, A., Arrighi, S., Badino, F., Bortolini, E., P., Boscato, Boschin, F., Crezzini, J., Delpiano, D., Falcucci., A., Figus, C., Lugli, F., Negrino, F., Oxilia G., Romandini, M., Riel-Salvatore, J., Spinapolice, E. E., Peresani, M., Moroni, A., Benazzi, S., this issue. Lithic techno-complexes in Italy from 50 to 39 thousand years BP: an overview of cultural and technological changes across the Middle-Upper Palaeolithic boundary.

Margari, V., Gibbard, P.L., Bryant, C.L., Tzedakis, P.C., 2009. Character of vegetational and environmental changes in southern Europe during the last glacial period; evidence from Lesvos Island, Greece. Quaternary Science Reviews, 28 (13-14), 1317-1339.

Margherita, C., Oxilia, G., Barbi, V., Panetta, D., Hublin, J-J., Lordkipanidze, D., Meshveliani, T., Jakeli, N., Matskevich Z., Bar-Yosef, O., Belfer-Cohen, A., Pinhasi, R., Benazzi, S., 2017. Morphological description and morphometric analyses of the Upper Palaeolithic human remains from Dzudzuana and Satsurblia caves, western Georgia. Journal of human evolution, 113, 83-90.

Mariani, G.S., Cremaschi, M., Zerboni, A., Zuccoli, L., Trombino, L., 2018. Geomorphological map of the Mt. Cusna Ridge (Northern Apennines, Italy): evolution of a Holocene landscape. Journal of Maps 14, 392–401.

Marković, S.B., Stevens, T., Kukla, G.J., Hambach, U., Fitzsimmons, K.E., Gibbard, P., Buggle, B., Zech, M., Guo, Z., Hao, Q., Wu, H., O'Hara Dhand, K., Smalley, I.J., Újvári, G., Sümegi, P., Timar-Gabor, A., Veres, D., Sirocko, F., Vasiljević, D.A., Jary, Z., Svensson, A., Jović, V., Lehmkuhl, F., Kovács, J., Svirčev, Z., 2015. Danube loess stratigraphy - Towards a pan-European loess stratigraphic model. Earth-Science Reviews, 148, 228–258.

1351 Marti, A., Folch, A., Costa, A., Engwell, S., 2016. Reconstructing the plinian and co-
1352 ignimbrite sources of large volcanic eruptions: A novel approach for the Campanian
1353 Ignimbrite. Scientific reports, 6, 21220.

1354 Martrat, B., Grimalt, J.O., Shackleton, N.J., de Abreu, L., Hutterli, M.A., Stocker, T.F.,
1355 2007. Four climate cycles of recurring deep and surface water destabilizations on the
1356 Iberian margin. Science, 317 (5837), 502-507.

1357 Maselli, V., Trincardi, F., Asioli, A., Ceregato, A., Rizzetto, F., Taviani, M., 2014. Delta
1358 growth and river valleys: the influence of climate and sea level changes on the South
1359 Adriatic shelf (Mediterranean Sea). Quaternary Science Reviews, 99, 146-163.

1360 McDermott, F., 2004. Palaeo-climate reconstruction from stable isotope variations in
1361 speleothems: a review. Quaternary Science Reviews, 23 (7-8), 901-918.

1362 McManus, J.F., Oppo, D.W., Cullen, J.L., 1999. A 0.5-million-year record of millennial
1363 scale climate variability in the North Atlantic. Science, 283 (5404), 971-975.

1364 Mellars, P., 2006. Archeology and the dispersal of modern humans in Europe:
1365 Deconstructing the “Aurignacian”. Evolutionary Anthropology: Issues, News, and Reviews:
1366 Issues, News, and Reviews, 15 (5), 167-182.

1367 Mihailović, D., Whallon, R., 2017. Crvena Stijena revisited: the late Mousterian
1368 assemblages. Quaternary International, 450, 36-49.

1369 Miko, S., Ilijanić, N., Hasan, O., Razum, I., Durn, T., Brunović, D., Papatheodorou, G.,
1370 Bakrač, K., Hajek, Tadesse, V., Šparica Miko, M., Crmarić, R., 2017. Submerged karst
1371 landscapes of the Eastern Adriatic. In 5th Regional Scientific Meeting on Quaternary
1372 Geology Dedicated to Geohazards and Final conference of the LoLADRIA project
1373 “Submerged Pleistocene landscapes of the Adriatic Sea”.

1374 Moine, O., Antoine, P., Hatté, C., Landais, A., Mathieu, J., Prud'homme, C., Rousseau, D.-
1375 D., 2017. The impact of Last Glacial climate variability in west-European loess revealed by
1376 radiocarbon dating of fossil earthworm granules. PNAS, 114 (24), 6209-6214.

1377 Monegato, G., Ravazzi, C., Donegana, M., Pini, R., Calderoni, G., Wick, L., 2007.
1378 Evidence of a two-fold glacial advance during the last glacial maximum in the Tagliamento
1379 end moraine system (eastern Alps). Quaternary Research 68, 284–302.

1380 Monegato, G., 2012. Local glaciers in the Julian Prealps (NE Italy) during the Last Glacial
1381 Maximum. Alpine and Mediterranean Quaternary. 25 pp. 5–14.

1382 Monegato, G., Scardia, G., Hajdas, I., Rizzini, F., Piccin, A., 2017. The Alpine LGM in the
1383 boreal ice-sheets game. Scientific Reports, 7: 2078.

1384 Moreno, A., Stoll, H., Jiménez-Sánchez, M., Cacho, I., Valero-Garcés, B., Ito, E., Edwards,
1385 R.L., 2010. A speleothem record of glacial (25–11.6 kyr BP) rapid climatic changes from
1386 northern Iberian Peninsula. Global and Planetary Change, 71 (3-4), 218-231.

1387 Morley, M.W., Woodward, J.C., 2011. The Campanian Ignimbrite at Crvena Stijena
1388 rockshelter in Montenegro, Quaternary Research, 75, 683-696.

1389 Moroni, A., Boscato, P., Ronchitelli, A., 2013. What roots for the Uluzzian? Modern
1390 behaviour in Central-Southern Italy and hypotheses on AMH dispersal routes. Quaternary
1391 International, 316, 27-44.

1392 Moroni, A., Ronchitelli, A., Arrighi, S., Aureli, D., Bailey, Boscato, P., Boschin, F.,
1393 Capecchi, G., Crezzini, J., Douka, K., Marciani, G., Panetta, D., Ranaldo, F., Ricci, S.,
1394 Scaramucci, S., Spagnolo, V., Benazzi, S., Gambassini, P., 2018. Grotta del Cavallo
1395 (Apulia–Southern Italy). The Uluzzian in the mirror. Journal of Anthropological
1396 Sciences, 96, 1-36.

1397 Moseley, G. E., Spötl, C., Svensson, A., Cheng, H., Brandstätter, S., Edwards, R. L., 2014.
1398 Multi-speleothem record reveals tightly coupled climate between central Europe and
1399 Greenland during Marine Isotope Stage 3. Geology, 42 (12), 1043-1046.

1400 Müller, U.C., Pross, J., Bibus, E., 2003. Vegetation response to rapid climate change in
1401 Central Europe during the past 140,000 yr based on evidence from the Füramoos pollen
1402 record. Quaternary Research, 59 (2), 235-245.

1403 Müller, U.C., Pross, J., Tzedakis, P.C., Gamble, C., Kotthoff, U., Schmiedl, G., Wulf, S.,
1404 Christanis, K., 2011. The role of climate in the spread of modern humans into Europe.
1405 Quaternary Science Reviews, 30 (3-4), 273-279.

1406 Naughton, F., Sánchez Goñi, M.F., Kageyama, M., Bard, E., Duprat, J., Cortijo, E.,
1407 Desprat, S., Malaize´, B., Joly, C., Rostek, F., Turon, J.-L., 2009. Wet to dry climatic trend
1408 in north-western Iberia within Heinrich events. Earth and Planetary Science Letters, 284,
1409 329–342.

1410 NGRIP members: High-resolution record of Northern Hemisphere climate extending into
1411 the last interglacial period, 2004. Nature, 431, 147–151.

1412 Nigst, P. R., Haesaerts, P., Damblon, F., Frank-Fellner, C., Mallol, C., Viola, B.,
1413 Götzingerh, M., Nivena, L., Trnkai, G., Hublin, J. J., 2014. Early modern human settlement
1414 of Europe north of the Alps occurred 43,500 years ago in a cold steppe-type environment.
1415 Proceedings of the National Academy of Sciences, 111(40), 14394-14399.

1416 Obruchev, V.A., 1914. The problem of North African loess. Zemlevedenie, 4, 26–31 (in
1417 Russian).

1418 Oliva, M., Palacios, D., Fernández-Fernández, J.M., Rodríguez-Rodríguez, L., García-
1419 Ruiz, J.M., Andrés, N., Carrasco, R.M., Pedraza, J., Pérez-Alberti, A., Valcárcel, M.,
1420 Hughes, P.D., 2019. Late Quaternary glacial phases in the Iberian Peninsula. Earth Sc.
1421 Rev. 192, 564-600.

1422 Pailler, D., Bard, E., 2002. High frequency palaeoceanographic changes during the past
1423 140000 yr recorded by the organic matter in sediments of the Iberian Margin.
1424 Palaeogeography, Palaeoclimatology, Palaeoecology, 181 (4), 431-452.

1425 Pallàs, R., Rodés, A., Braucher, R., Bourlès, D., Delmas, M., Calvet, M., Gunnell, Y., 2010.
1426 Small isolated glacial catchments as priority targets for cosmogenic surface exposure
1427 dating of Pleistocene climate fluctuations, southeastern Pyrenees. Geology 38, 891–894.

1428 Palma di Cesnola, A., 1989. L'Uluzzien: faciès italien du Leptolithique archaïque.
1429 L'Anthropologie, 93 (4), 783-812.

1430 Palma di Cesnola, A., 2004. Paglicci. L'Aurignaziano e il Gravettiano antico.

1431 Panagiotopoulos, K., Böhm, A., Leng, M.J., Wagner, B., Schäbitz, F., 2014. Climate
1432 variability over the last 92 ka in SW Balkans from analysis of sediments from Lake Prespa.
1433 Climate of the Past, 10 (2), 643-660.

1434 Pellegrini, C., Maselli, V., Cattaneo, A., Piva, A., Ceregato, A., Trincardi, F., 2015.
1435 Anatomy of a compound delta from the post-glacial transgressive record in the Adriatic
1436 Sea. Marine Geology, 362, 43-59.

1437 Peresani, M., Cremaschi, M., Ferraro, F., Falgueres, C., Bahain, J.J., Gruppioni, G.,
1438 Sibilia, E., Quarta G., Calcagnile, L., Dolo, J. M., 2008. Age of the final Middle Palaeolithic
1439 and Uluzzian levels at Fumane Cave, Northern Italy, using 14C, ESR, 234U/230Th and
1440 thermoluminescence methods. Journal of Archaeological Science, 35 (11), 2986-2996.

1441 Peresani, M., 2011. The end of the Middle Palaeolithic in the Italian Alps. An overview on
1442 Neandertal land-use, subsistence and technology. In: Conards N. & Richter J. (eds.),
1443 Neanderthal lifeways, subsistence and technology. One Hundred Fifty Years of
1444 Neanderthal Study. Vertebrate Paleobiology and Paleoanthropology Series, Springer ed.,
1445 249-259.

1446 Peresani, M., 2014. L'Uluzzien en Italie. In: Otte, M. (Ed.), Néandertal/Cro-Magnon. La
1447 Rencontre. Editions Errance, Arles, 61-80.

1448 Peresani, M., Cristiani, E., Romandini, M., 2016. The Uluzzian technology of Grotta di
1449 Fumane and its implication for reconstructing cultural dynamics in the Middle–Upper
1450 Palaeolithic transition of Western Eurasia. Journal of human evolution, 91, 36-56.

1451 Peresani, M., Bertola, S., Delpiano, D., Benazzi, S., Romandini, M., 2018. The Uluzzian in
1452 the north of Italy: insights around the new evidence at Riparo Broion. Archaeological and
1453 Anthropological Sciences, 1-34.

1454 Peresani, M., Bertola, S., Delpiano, D., Benazzi, S., Romandini, M., 2019. The Uluzzian in
1455 the north of Italy: insights around the new evidence at Riparo Broion. Archaeological and
1456 Anthropological Sciences, 11, 3503-3536.

1457 Peters, C., Walden, J., Austin, W.E., 2008. Magnetic signature of European margin
1458 sediments: Provenance of ice-rafted debris and the climatic response of the British ice
1459 sheet during Marine Isotope Stages 2 and 3. Journal of Geophysical Research: Earth
1460 Surface, 113 (F3).

1461 Petersen, S.V., Schrag, D.P., Clark, P.U., 2013. A new mechanism for
1462 Dansgaard-Oeschger cycles. Paleoceanography, 28 (1), 24-30.

1463 Peterson, L.C., Haug, G.H., 2006. Variability in the mean latitude of the Atlantic
1464 Intertropical Convergence Zone as recorded by riverine input of sediments to the Cariaco
1465 Basin (Venezuela). Palaeogeography, Palaeoclimatology, Palaeoecology, 234 (1), 97-113.

1466 Pini, R., Ravazzi, C., Donegana, M., 2009. Pollen stratigraphy, vegetation and climate
1467 history of the last 215 ka in the Azzano Decimo core (plain of Friuli, north-eastern Italy).
1468 Quaternary Science Reviews, 28, 1268-1290.

1469 Pini, R., Ravazzi, C., Reimer P.J., 2010. The vegetation and climate history of the last
1470 glacial cycle in a new pollen record from Lake Fimon (southern Alpine foreland, N-Italy).
1471 Quaternary Science Reviews, 29: 3115-3137.

1472 Popescu, R., Urdea, P., Vespremeanu-Stroe, A., 2017. Deglaciation History of High
1473 Massifs from the Romanian Carpathians: Towards an Integrated View. In: M. Rădoane
1474 and A. Vespremeanu-Stroe (eds.), Landform Dynamics and Evolution in Romania,
1475 Springer Geography, 87-116.

1476 Pross, J., Koutsodendris, A., Christanis, K., Fischer, T., Fletcher, W.J., Hardiman, M.,
1477 Kalaitzidis, S., Knipping, M., Kotthoff, U., Milner, A.M., Müller, U.C., Schmiedl, G.,
1478 Siavalas, G., Tzedakis, P.C., Wulf, S., 2015. The 1.35-Ma-long terrestrial climate archive
1479 of Tenaghi Philippon, northeastern Greece: Evolution, exploration, and perspectives for
1480 future research. Newsletters on Stratigraphy, 48 (3), 253-276.

1481 Pye, K., 1995. The nature, origin and accumulation of loess. Quaternary Science Reviews,
1482 14, 653–667.

1483 Pyle, D.M., Ricketts, G.D., Margari, V., van Andel, T.H., Sinitsyn, A.A., Praslov, N.D.,
1484 Lisitsyn, S., 2006. Wide dispersal and deposition of distal tephra during the Pleistocene
1485 'Campanian Ignimbrite/Y5' eruption, Italy. Quaternary Science Reviews, 25, 2713–2728.

1486 Rasmussen, S.O., Andersen, K.K., Svensson, A.M., Steffensen, J.P., Vinther, B.M.,
1487 Clausen, H.B., Siggaard-Andersen, M.-L., Johnsen S. J., Larsen, L. B., Dahl-Jensen, D.,
1488 Bigler, M., Röthlisberger, R., Fischer, H., Goto-Azuma K., Hansson, M.E., Ruth, U., 2006.
1489 A new Greenland ice core chronology for the last glacial termination. Journal of
1490 Geophysical Research: Atmospheres, 111 (D6).

1491 Rasmussen, S.O., Bigler, M., Blockley, S.P., Blunier, T., Buchardt, S.L., Clausen, H.B.,
1492 Cvijanovic, I., Dahl-Jensen, D., Johnsen, S.J., Fischer, H., 2014. A stratigraphic framework
1493 for abrupt climatic changes during the Last Glacial period based on three synchronized

1494 Greenland ice-core records: refining and extending the INTIMATE event stratigraphy.
1495 Quaternary Science Reviews, 106, 14-28.

1496 Ravazzi, C., Peresani, M., Pini, R., Vescovi, E., 2007. Il Tardoglaciale nelle Alpi italiane e
1497 in Pianura Padana. Evoluzione stratigrafica, storia della vegetazione e del popolamento
1498 antropico. Il Quaternario, 20 (2), 163-184.

1499 Ravazzi, C., Badino, F., Marsetti, D., Patera, G., Reimer, P., 2012. Glacial to paraglacial
1500 history and forest recovery in the Oglio glacier system (Italian Alps) between 26 and 15 ka
1501 cal BP. Quaternary Science Reviews, 58, 146–161.

1502 Reber, R., Akçar, N., Ivy-Ochs, S., Tikhomirov, D., Burkhalter, R., Zahno, C., Lüthold, A.,
1503 Kubik, P.W., Vockenhuber, C., Schlüchter, C., 2014. Timing of retreat of the Reuss glacier
1504 (Switzerland) at the end of the last glacial maximum. Swiss Journal of Geosciences 107,
1505 293–307.

1506 Reille, M., Beaulieu, J.L. de, 1990. Pollen analysis of a long upper Pleistocene continental
1507 sequence in a Velay maar (Massif Central, France). Palaeogeography, Palaeoclimatology,
1508 Palaeoecology, 80 (1), 35-48.

1509 Rey-Rodríguez, I., López-García, J.M., Bennasar, M., Bañuls-Cardona, S., Blain, H.A.,
1510 Blanco-Lapaz, Á., Rodríguez-Álvarez, X.-P., de Lombera-Hermida, A., Díaz-Rodríguez,
1511 M., Ameijenda-Iglesias, A., Agustí, J., Fábregas-Valcarce, R., 2016. Last Neanderthals
1512 and first Anatomically Modern Humans in the NW Iberian Peninsula: Climatic and
1513 environmental conditions inferred from the Cova Eirós small-vertebrate assemblage during
1514 MIS 3. Quaternary Science Reviews 151, 185-197.

1515 Riel-Salvatore, J., Negrino, F., 2018. Human adaptations to climatic change in Liguria
1516 across the Middle–Upper Paleolithic transition. Journal of Quaternary Science, 33 (3), 313-
1517 322.

1518 Roche, D., Paillard, D., Cortijo, E., 2004. Constraints on the duration and freshwater
1519 release of Heinrich event 4 through isotope modelling. Nature, 432 (7015), 379.

1520 Ronchitelli, A., Boscato, P., Gambassini, P., 2009. Gli ultimi Neandertaliani in Italia: aspetti
1521 culturali. In: Facchini, F., Belcastro, G. (Eds.), La lunga storia di Neandertal. Biologia e
1522 comportamento. Jaka Book, Bologna, Italy, 257-288.

1523 Rossato, S., Monegato, G., Mozzi, P., Cucato, M., Gaudioso, B., Miola, A., 2013. Late
1524 Quaternary glaciations and connections to the piedmont plain in the prealpine
1525 environment: the middle and lower Astico Valley (NE Italy). Quat. Int. 288, 8–24.

1526 Rossato, S., Carraro, A., Monegato, G., Mozzi, P., Tateo, F., 2018. Glacial dynamics in
1527 pre-Alpine narrow valleys during the Last Glacial Maximum inferred by lowland fluvial
1528 records (northeast Italy). Earth Surface Dynamics 6, 809-828.

1529 Roucoux, K. H., De Abreu, L., Shackleton, N. J., Tzedakis, P. C., 2005. The response of
1530 NW Iberian vegetation to North Atlantic climate oscillations during the last 65 kyr.
1531 Quaternary Science Reviews, 24(14-15), 1637-1653.

1532 Rousseau, D.-D., Derbyshire, E., Antoine, P., Hatté, C., 2018. European Loess Records.
1533 Reference Module in Earth Systems and Environmental Sciences, 1-17.

1534 Ruddiman, W.F., 1977. Late Quaternary deposition of ice-rafted sand in the subpolar
1535 North Atlantic (lat 40 to 65 N). Geological Society of America Bulletin, 88 (12), 1813-1827.

1536 Ruszkiczay-Rüdiger, Z., Kern, Z., Urdea, P., Braucher, R., Madarász, B.,
1537 Schimmelpfennig, I., 2016. Revised deglaciation history of the Pietrele-Stâni¸soara glacial
1538 complex, Retezat Mts, Southern Carpathians, Romania. Quaternary International, 415,
1539 216–229.

1540 Ruth, U., Bigler, M., Röthlisberger, R., Siggaard-Andersen, M.L., Kipfstuhl, S.,
1541 Goto-Azuma, K., Hansson, M.E., Johnsen, S. J., Lu, H., Steffensen, J.P., 2007. Ice core

1542 evidence for a very tight link between North Atlantic and east Asian glacial climate.
1543 Geophysical Research Letters, 34 (3).

1544 Sadori, L., Koutsodendris, A., Panagiotopoulos, K., Masi, A., Bertini, A., Combourieu-
1545 Nebout, N., Francke, A., Kouli, K., Joannin, S., Mercuri, A.M., Peyron, O., Torri, P.,
1546 Wagner, B., Zanchetta, G., Sinopoli G., Donders, T.H., 2016. Pollen-based
1547 paleoenvironmental and paleoclimatic change at Lake Ohrid (south-eastern Europe)
1548 during the past 500 ka. Biogeosciences, 13 1423-1437.

1549 Salcher, B. C., Starnberger, R., Götz, J., 2015. The last and penultimate glaciation in the
1550 North Alpine Foreland: New stratigraphical and chronological data from the Salzach
1551 glacier. Quat. Int. 388, 218-231.

1552 Sánchez Goñi, M.F., Eynaud, F., Turon, J.L., Shackleton, N.J., 1999. High resolution
1553 palynological record off the Iberian margin: direct land-sea correlation for the Last
1554 Interglacial complex. Earth and Planetary Science Letters, 171 (1), 123-137.

1555 Sánchez Goñi, M.F., Turon, J.L., Eynaud, F., Gendreau, S., 2000. European climatic
1556 response to millennial-scale changes in the atmosphere–ocean system during the Last
1557 Glacial period. Quaternary Research, 54 (3), 394-403.

1558 Sánchez Goñi, M.F., Cacho, I., Turon, J., Guiot, J., Sierro, F., Peypouquet, J., Grimalt, J.,
1559 Shackleton, N., 2002. Synchroneity between marine and terrestrial responses to millennial
1560 scale climatic variability during the last glacial period in the Mediterranean region. Climate
1561 Dynamics, 19 (1), 95-105.

1562 Sánchez Goñi, M.F., Landais, A., Fletcher, W.J., Naughton, F., Desprat, S., Duprat, J.,
1563 2008. Contrasting impacts of Dansgaard–Oeschger events over a western European
1564 latitudinal transect modulated by orbital parameters. Quaternary Science Reviews, 27 (11),
1565 1136-1151.

1566 Sánchez Goñi, M.F., Landais, A., Cacho, I., Duprat, J., Rossignol, L., 2009. Contrasting
1567 intrainterstadial climatic evolution between high and middle North Atlantic latitudes: A
1568 close-up of Greenland Interstadials 8 and 12. Geochemistry, Geophysics, Geosystems, 10
1569 (4).

1570 Satow, C., Tomlinson, E.L., Grant, K.M., Albert, P.G., Smith, V.C., Manning, C.J., Ottolini,
1571 L., Wulf, S., Rohling, E.J., Lowe, J.J., Blockley, S.P.E., Menzies, M.A., 2015. A new
1572 contribution to the Late Quaternary tephrostratigraphy of the Mediterranean: Aegean Sea
1573 core LC21. Quaternary Science Reviews, 117, 96-112.

1574 Schneider, U., Becker, A., Finger, P., Meyer-Christoffer, A., Ziese, M., Rudolf, B., 2014.
1575 GPCC's new land surface precipitation climatology based on quality-controlled in situ data
1576 and its role in quantifying the global water cycle, Theoretical and Applied Climatology, 115,
1577 1–15.

1578 Seguinot, J., Ivy-Ochs, S., Jouvet, G., Huss, M., Funk, M., Preusser, F., 2018. Modelling
1579 last glacial cycle ice dynamics in the Alps. The Cryosphere, 12, 3265-3285.

1580 Seierstad, I.K., Abbott, P.M., Bigler, M., Blunier, T., Bourne, A.J., Brook, E., Buchardt, S.,
1581 L., Buizert, C., Clausen, H.B., Cook E., Dahl-Jensen, D., Davies, S.M., Guillevic, M.,
1582 Johnsen, S.J., Pedersen, D.S., Popp, T.J., Rasmussen, S.O., Severinghaus, J.P.,
1583 Svensson, A., Vinther, B.M., 2014. Consistently dated records from the Greenland GRIP,
1584 GISP2 and NGRIP ice cores for the past 104 ka reveal regional millennial-scale $\delta^{18}O$
1585 gradients with possible Heinrich event imprint. Quaternary Science Reviews, 106, 29-46.

1586 Seret, G., Dricot, E., Wansard, G. 1990. Evidence for an early glacial maximum in the
1587 French Vosges during the last glacial cycle. Nature 346, 453-456.

1588 Serrano, E., Gómez-Lende, M., González-Amuchastegui, M.J., González-García, M.,
1589 González-Trueba, J.J., Pellitero, R., Rico, I., 2015. Glacial chronology, environmental
1590 changes and implications for human occupation during the upper Pleistocene in the
1591 eastern Cantabrian Mountains. Quaternary International 364, 22–34.

1592 Sirocko, F., Knapp, H., Dreher, F., Förster, M.W., Albert, J., Brunck, H., Veres, D., Dietrich,
1593 S., Zech, M., Hambach, U., Röhner, M., Rudert, S., Schwibus, K., Adams, C., Sigl, P.,
1594 2016. The ELSA-Vegetation-Stack: Reconstruction of Landscape Evolution Zones (LEZ)
1595 from laminated Eifel maar sediments of the last 60,000 years. Global and Planetary
1596 Change, 142, 108-135.

1597 Smalley, I.J., Leach, J.A., 1978. The origin and distribution of the loess in the Danube
1598 basin and associated regions of East-Central Europe e a review. Sedimentary Geology,
1599 21, 1–26.

1600 Spennato, A.G., 1981. I livelli protoaurignaziani della Grotta di Serra Cicora. Studi per
1601 l'Ecologia del Quaternario 61, 52–76.

1602 Spötl, C., Mangini, A., Frank N., Eichstädter, R., Burns, S.J., 2002. Start of the Last
1603 Interglacial period at 135 ka: evidence from a high alpine speleothem. Geology 30 (9),
1604 815-818.

1605 Spötl, C., Mangini, A., 2007. Speleothems and paleoglaciers. Earth and Planetary Science
1606 Letters, 254 (3-4), 323-331.

1607 Staff, R. A., Hardiman, M., Ramsey, C. B., Adolphi, F., Hare, V. J., Koutsodendris, A.,
1608 Pross, J., 2019. Reconciling the Greenland ice-core and radiocarbon timescales through
1609 the Laschamp geomagnetic excursion. Earth and Planetary Science Letters, 520, 1-9.

1610 Starkovich, B.M., 2017. Paleolithic subsistence strategies and changes in site use at
1611 Klissoura Cave 1 (Peloponnese, Greece). Journal of human evolution, 111, 63-84.

1612 Staubwasser, M., Drăgușin, V., Onac, B.P., Assonov, S., Ersek, V., Hoffmann, D.L., Veres,
1613 D., 2018. Impact of climate change on the transition of Neanderthals to modern humans in
1614 Europe. Proceedings of the National Academy of Sciences, 115 (37), 9116-9121.

1615 Steegmann Jr., A.T., Cerny, F.J., Holliday, T.W., 2002. Neandertal cold adaptation:
1616 physiological and energetic factors. American Journal of Human Biology, 14 (5), 566-583.

1617 Steffensen, J.P., Andersen, K.K., Bigler, M., Clausen, H. B., Dahl-Jensen, D., Fischer, H.,
1618 Goto-Azuma, K., Hansson M., Johnsen, S.J., Jouzel, J., Masson-Delmotte, V., Popp, T.,
1619 Rasmussen, S.O., Röthlisberger, R., Ruth, U., Stauffer B., Siggaard-Andersen, M.-L.,
1620 Sveinbjörnsdóttir, A., E., Svensson, A., White, J.W.C., 2008. High-resolution Greenland ice
1621 core data show abrupt climate change happens in few years. Science, 321 (5889), 680-
1622 684.

1623 Stern, J.V., Lisiecki, L.E., 2013. North Atlantic circulation and reservoir age changes over
1624 the past 41,000 years. Geophysical Research Letters, 40 (14), 3693-3697.

1625 Stiner, M.C., Kozowski, J.K., Kuhn, S.L., Karkanas, P., Koumouzelis, M., 2007. Klissoura
1626 Cave 1 and the Upper Paleolithic of Southern Greece in Cultural and Ecological Context.
1627 Eurasian Prehistory 7, 309–321.Stoll, H.M., Moreno, A., Mendez-Vicente, A., Gonzalez-
1628 Lemos, S., Jimenez-Gochez, M., Dominguez-Cuesta, M.J., Edwards, R.L., Cheng. H.,
1629 Wang, X., 2013. Paleoclimate and growth rates of speleothems in the northwestern Iberian
1630 Peninsula over the last two glacial cycles. Quaternary Research, 80 (2), 284-290.

1631 Svensson, A., Andersen, K.K., Bigler, M., Clausen, H.B., Dahl-Jensen, D., Davies, S.M.,
1632 Johnsen, S.J., Muscheler, R., Parrenin, F., Rasmussen, S.O., Röthlisberger, R., Seierstad,
1633 I., Steffensen, J.P., Vinther, B.M., 2008. A 60,000 year Greenland stratigraphic ice core
1634 chronology. Climate of the Past, 4, 47–57.

1635 Temovski, M., Madarász, B., Kern, Z., Milevski, I., Ruszkiczay-Rüdiger, Z., 2018. Glacial
1636 Geomorphology and Preliminary Glacier Reconstruction in the Jablanica Mountain,
1637 Macedonia, Central Balkan Peninsula. Geosciences 8, 270.
1638 doi:10.3390/geosciences8070270.

1639 Terhorst, B., Sedov, S., Sprafke, T., Peticzka, R., Meyer-Heintze, S., Kühn, P., Solleiro
1640 Rebolledo, E., 2015. Austrian MIS 3/2 loess–palaeosol records-Key sites along a west–
1641 east transect. Palaeogeography, Palaeoclimatology, Palaeoecology, 418, 43–56.

1642 Thiel, C., Horváth, E., Frechen, M., 2014. Revisiting the loess/palaeosol sequence in Paks,
1643 Hungary: a post-IR IRSL based chronology for the 'Young Loess Series'. Quaternary
1644 International, 319, 88–98

1645 Timar, A., Vandenberghe, D., Panaiotu, E.C., Panaiotu, C.G., Necula, C., Cosma, C., van
1646 den Haute, P., 2010. Optical dating of Romanian loess using fine-grained quartz.
1647 Quaternary Geochronology, 5 (2-3), 143–148.

1648 Timar-Gabor, A., Vandenberghe, D.A.G., Vasiliniuc, S., Panaoitu, C.E., Panaiotu, C.G.,
1649 Dimofte, D., Cosma, C., 2011. Optical dating of Romanian loess: a comparison between
1650 silt-sized and sand-sized quartz. Quaternary International, 240, 62–70.

1651 Tinner, W., Hubschmid, P., Wehrli, M., Ammann, B., Conedera, M., 1999. Long-term forest
1652 fire ecology and dynamics in southern Switzerland. Journal of Ecology, 87, 273-289.

1653 Toucanne, S., Soulet, G., Freslon, N., Jacinto, R.S., Dennielou, B., Zaragosi, S. Eynaud;
1654 F., Bourillet, J.-F., Bayon, Germain., 2015. Millennial-scale fluctuations of the European
1655 Ice Sheet at the end of the last glacial, and their potential impact on global climate.
1656 Quaternary Science Reviews, 123, 113-133.

1657 Tranquillini, W., 1979. General Features of the Upper Timberline. In Physiological Ecology
1658 of the Alpine Timberline. Springer Berlin Heidelberg, 1-4.

1659 Turkish State Meteorological Service, 2006. Climate of Turkey. Turkish State
1660 Meteorological Service. Archived from the original on April 19, 2008. Retrieved 2006-12-
1661 27.

1662 Tzedakis, P. C., 1999. The last climatic cycle at Kopais, central Greece. Journal of the
1663 Geological Society, 156 (2), 425-434.

1664 Tzedakis, P.C., Lawson, I.T., Frogley, M.R., Hewitt, G.M., Preece, R.C., 2002. Buffered
1665 tree population changes in a Quaternary refugium: evolutionary implications. Science, 297
1666 (5589), 2044-2047.

1667 Tzedakis, P. C., Frogley, M. R., Lawson, I. T., Preece, R. C., Cacho, I., De Abreu, L.,
1668 2004. Ecological thresholds and patterns of millennial-scale climate variability: the
1669 response of vegetation in Greece during the last glacial period. Geology, 32 (2), 109-112.

1670 Tzedakis, P.C., Hooghiemstra, H., Pälike, H., 2006. The last 1.35 million years at Tenaghi
1671 Philippon: revised chronostratigraphy and long-term vegetation trends. Quaternary
1672 Science Reviews, 25 (23-24), 3416-3430.

1673 Valen, V., Larsen, E., Mangerud, J.A.N., 1995. High-resolution paleomagnetic correlation
1674 of Middle Weichselian ice-dammed lake sediments in two coastal caves, western
1675 Norway. Boreas, 24 (2), 141-153.

1676 van Andel, T.H., Tzedakis P.C., 1998. Priority and opportunity: reconstructing the
1677 European Middle Palaeolithic climate and landscape. In (Bailey, J., ed.): Science in
1678 Archaeology. An agenda for the future. English Heritage, 37-45.

1679 van Andel, T.H., Davies, W., Weninger, B., 2003. The human presence in Europe during
1680 the last glacial period I: human migrations and the changing climate. Neanderthals and
1681 modern humans in the European landscape during the last glaciation: archaeological
1682 results of the Stage, 3, 31-56.

1683 Van Meerbeeck, C.J., Renssen, H., Roche, D.M., Wohlfarth, B., Bohncke, S.J.P., Bos,
1684 J.A.A., Engels, S., Helmens, K.F., Sánchez Goñi, F., Svensson, A., Vandenberghe J.,
1685 2011. The nature of MIS 3 stadial-interstadial transitions in Europe: new insights from
1686 model-data comparison. Quaternary Science Reviews, 30, 3618-3637.

1687 Verheul, J., Zickel, M., Becker, D., Willmes, C., 2015. LGM major inland waters of Europe-
1688 GIS dataset. CRC806-Database, DOI: http://dx. doi. org/10.5880/SFB806, 14.

1689 Villa, P., Roebroeks, W., 2014. Neandertal demise: An archaeological analysis of the
1690 modern human superiority complex. PLoS ONE, 9(4), e96424.

1691 Wacha, L., Pavlaković, S.M., Frechen, M., Crnjaković, M., 2011a. The Loess chronology of
1692 the Island of Susak, Croatia. E&G Quaternary Science Journal, 60, 153–169.

1693 Wacha, L., Pavlakovic, S., Novothny, A., Crnjaković, M., Frechen, M., 2011b.
1694 Luminescence dating of Upper Pleistocene loess from the Island of Susak in Croatia.
1695 Quaternary International, 234, 50–61.

1696 Waelbroeck, C., Labeyrie, L., Michel, E., Duplessy, J. C., Lambeck. K., McManus, J. F.,
1697 Balbon, E., Labracherie, M., 2002. Sea-level and deep water temperature changes derived
1698 from benthic foraminifera isotopic records. Quaternary Science Reviews, 21, 295-305.

1699 Wainer, K., Genty, D., Blamart, D., Hoffmann, D., Couchoud, I., 2009. A new stage 3
1700 millennial climatic variability record from a SW France speleothem. Palaeogeography,
1701 Palaeoclimatology, Palaeoecology, 271 (1), 130-139.

1702 Walter, H., Breckle, S.W., 1986. Spezielle Ökologie der gemässigten und arktischen
1703 Zonen Euro-Nordasiens: Zonobiom VI-IX. Fischer.

1704 Weber, M., Scholz, D., Schröder-Ritzrau, A., Deininger, M., Spötl, C., Lugli, F., Mertz-
1705 Kraus, R., Jochum, K.P., Fohlmeister, J., Stumpf, C.F., Riechelmann, D.F.C., 2018.
1706 Evidence of warm and humid interstadials in central Europe during early MIS 3 revealed
1707 by a multi-proxy speleothem record. Quaternary Science Reviews, 200, 276-286.

1708 Whitlock, C., Larsen, C., 2001. Charcoal as a fire proxy. Smol, JP, Birks, HJB and Last,
1709 WM (eds.) Tracking environmental change using lake sediments Vol. 3, Terrestrial, algal,
1710 and Siliceous Indicators, 75-97.

1711 Whitlock, C., Larsen, C., 2001. Charcoal as a fire proxy. Smol, JP, Birks, HJB and Last,
1712 WM (eds.) Tracking environmental change using lake sediments Vol. 3, Terrestrial, algal,
1713 and Siliceous Indicators, 75-97.

1714 Wijmstra, T.A., 1969. Palynology of the first 30 metres of a 120 m deep section in northern
1715 Greece. Acta Botanica Neerlandica, 18 (4), 511-527.

1716 Wohlfarth, B., 2010. Ice-free conditions in Sweden during Marine Oxygen Isotope Stage
1717 3?. Boreas, 39 (2), 377-398.

1718 Woillard, G.M., 1978. Grande Pile peat bog: a continuous pollen record for the last
1719 140,000 years. Quaternary Research, 9, 1-21.

1720 Wood, R. E., Douka, K., Boscato, P., Haesaerts, P., Sinitsyn, A., Higham, T., 2012.
1721 Testing the ABOx-SC method: dating known-age charcoals associated with the
1722 Campanian Ignimbrite. Quaternary Geochronology, 9, 16-26.

1723 Wood, R., 2015. From revolution to convention: the past, present and future of radiocarbon
1724 dating. Journal of Archaeological Science, 56, 61-72.

1725 Wroe, S., Parr, W.C., Ledogar, J.A., Bourke, J., Evans, S.P., Fiorenza, L., Benazzi, S.,
1726 Hublin, J.-J., Stringer C., Kullmer, O., Curry, M., Rae, T.C., Yokley, T.R., 2018. Computer
1727 simulations show that Neanderthal facial morphology represents adaptation to cold and
1728 high energy demands, but not heavy biting. Proceedings Royal Society B, 285 (1876),
1729 20180085.

1730 Wulf, S., Hardiman, M. J., Staff, R.A., Koutsodendris, A., Appelt, O., Blockley, S.P., Lowe,
1731 J.J., Manning C.J., Ottolini, L., Schmitt, A.K., Smith, V.C., Tomlinson E.L., Vakhrameeva,
1732 P., Knipping, M., Kotthoff, U., Milner, A.M., Müller, U.C., Christanis K., Kalaitzidis S.,
1733 Tzedakis, P.C., Schmiedl G., Pross J., 2018. The marine isotope stage 1–5 cryptotephra
1734 record of Tenaghi Philippon, Greece: Towards a detailed tephrostratigraphic framework for
1735 the Eastern Mediterranean region. Quaternary Science Reviews, 186, 236-262.

1736 Wutke, K., Wulf, S., Tomlinson, E. L., Hardiman, M., Dulski, P., Luterbacher, J., Brauer, A.,
1737 2015. Geochemical properties and environmental impacts of seven Campanian tephra
1738 layers deposited between 40 and 38 ka BP in the varved lake sediments of Lago Grande
1739 di Monticchio, southern Italy. Quaternary Science Reviews, 118, 67-83.

1740 Yazbeck, C., 2004. Le Paleolithique du Liban: bilan critique. Paleorient, 30, 111-126.

1741 Zanchetta, G., Giaccio, B., Bini, M., Sarti, L., 2018. Tephrostratigraphy of Grotta del
1742 Cavallo, Southern Italy: Insights on the chronology of Middle to Upper Palaeolithic
1743 transition in the Mediterranean. Quaternary Science Reviews, 182, 65-77.

1744 Zasadni, J., Klapyta, P., 2014. The Tatra Mountains during the Last Glacial Maximum.
1745 Journal of Maps, 10 (3), 440-456.

1746 Žebre, M., Stepišnik, U., 2014. Reconstruction of Late Pleistocene glaciers on Mount
1747 Lovćen, Montenegro. Quaternary International, 353, 225–235.

1748 Žebre, M., Stepišnik, U., 2015. Glaciokarst geomorphology of the northern Dinaric alps:
1749 Snežnik (Slovenia) and Gorski Kotar (Croatia). Journal of Maps 5, 873-881.
1750 doi.org/10.1080/17445647.2015.1095133.

1751 Žebre, M., Stepišnik, U., Colucci, R.R., Forte, E., Monegato, G., 2016. Evolution of a karst
1752 polje influenced by glaciation: the Gomance piedmont polje (northern Dinaric Alps).
1753 Geomorphology, 257, 143–154.

1754 Žebre, M., Jež, J., Mechernich, S., Mušič, B., Horn, B., Jamšek Rupnik, P., 2019.
1755 Paraglacial adjustment of alluvial fans to the last deglaciation in the Snežnik Mountain,
1756 Dinaric karst (Slovenia). Geomorph. 332, 66-79.

1757 Zerboni, A., Trombino, L., Frigerio, C., Livio, F., Berlusconi, A., Michetti, A.M., Rodnight,
1758 H., Spötl, C., 2015. The loess -paleosol sequence at Monte Netto: a record of climate

change in the Upper Pleistocene of the central Po Plain, northern Italy. Journal of Soils and Sediments, 15, 1329-1350.

Zerboni, A., Amit, R., Baroni, C., Coltorti, M., Ferrario, M.F., Fioraso, G., Forno, M.G., Frigerio, C., Gianotti, F., Irace, A., Livio, F., Mariani, G.S., Michetti, A.M., Monegato, G., Mozzi, P., Orombelli, G., Perego, A., Porat, N., Rellini, I., Trombino, L., Cremaschi, M., 2018. Towards a map of the Upper Pleistocene loess of the Po Plain Loess Basin (Northern Italy). Alpine and Mediterranean Quaternary, 31, 253–256.

Zhornyak, L.V., Zanchetta, G., Drysdale, R. N., Hellstrom, J.C., Isola, I., Regattieri, E., Piccini, L., Baneschi, I., Couchoud, I., 2011. Stratigraphic evidence for a “pluvial phase” between ca 8200–7100 ka from Renella cave (Central Italy). Quaternary Science Reviews, 30 (3-4), 409-417.

Zilhão, J, Bank,s W.E., d’Errico, F., Gioia. P., 2015. Analysis of site formation and assemblage integrity does not support attribution of the Uluzzian to modern humans at Grotta del Cavallo. PLosOne 10(7): e0131181.

Figure captions

Fig. 1 Comparison of Northern Hemisphere terrestrial and marine paleoclimate proxies: (a) NGRIP $\delta^{18}O$ record (Rasmussen et al., 2014), (b) temperature reconstruction based on $\delta^{15}N$ (Kindler et al., 2014) and (c) calcium ion concentration ($[Ca^{2+}]$) record (Rasmussen et al 2014), plotted all on the GICC05modelext chronology (Rasmussen et al., 2014); (d) NEEM ^{17}O-excess permeg (Guillevic et al., 2014); (e) $\delta^{18}O$ record from Northern Alps (NALPS) speleothems (Moseley et a., 2014) plotted on its timescale; (f) MD95-2042 Sea Surface Temperature record (Darfeuil et al., 2016), (g) *Neogloboquadrina pachyderma*

1784 abundance and (h) Ice-Radfted Debris record (Sánchez Goñi et al., 2008), plotted each on
1785 their own timescale. Vertical grey bars indicate Greenland Stadial (GS). Heinrich events
1786 (HEs) are indicated according to MD95-2042 chronology (Sánchez Goñi et al., 2008).

1787

1788 **Fig. 2** European biogeographical map. Overview of mid- to high-resolution marine and
1789 terrestrial records entirely or partially covering MIS 3.

1790

1791 **Fig. 3** Vegetation changes throughout MIS 3 in several high- to mid-resolution terrestrial
1792 pollen records from S-Europe and Mediterranean region. Pollen curves: % of woody taxa
1793 (sum of trees and shrubs) (light green); % of arboreal pollen (dark green); % of xerophytic
1794 elements (sum of *Artemisia* and Chenopodiaceae) (grey). Black histograms show pollen-
1795 slide microcharcoal concentrations. All records are plotted using the latest available
1796 chronology for each individual site. NGRIP $\delta^{18}O$ record is also shown (NGRIP members,
1797 2004; Rasmussen et al., 2014). Red numbers indicate Greenland Interstadials (GI),
1798 modified from Fletcher et al., 2010. Heinrich events (HEs) are indicated according to
1799 MD95-2042 chronology (Sánchez Goñi et al., 2008).

1800

1801 **Fig. 4 - A)** Ecogeography of Greenland Interstadial 12 (GI 12; ca. 46.8 to 44.2 ka
1802 according to Rassmussen et al., 2014), showing reconstructed gradients within European
1803 eco-climatic zones. Digital Elevation Model (base topography – ETOPO 2011;
1804 ETRS_1989_LAEA_152 projected coordinate system). Sea surface lowered to -74 m asl
1805 (Waelbroeck et al., 2002; Antonioli, 2012). Baltic lake drawn after Lambeck et al., 2010.
1806 The mountain glaciers (pale blue) and the main Alpine valley glaciers (cyan triangles) are
1807 inferred both from simulations (Seguinot et al., 2018) and ELA calculations, for more
1808 information see section 4.1.2. Colour scale bars depict eco-climatic zones gradients.
1809 Sharp limits mark reconstructed elevational timberlines position and mountain glaciers
1810 extent in different mountain systems within each eco-climatic zone, see sections 4.1 and
1811 4.2. **B)** Palaeogeographic map of Europe during the Last Glacial Maximum. Digital

Elevation Model (base topography – ETOPO 2011; ETRS_1989_LAEA_152 projected coordinate system). Sea level drop at – 120 m (Pellegrini et al., 2015; Maselli et al 2014). Scandinavian and British Islands ice sheets (pale blue) after Hughes et al. (2016) at 22 ka. The mountain glaciers (pale blue) from Ehlers et al. (2011) with updated reconstructions in the Tatra Mountains (Zasadni and Klapyta, 2014), Dinarides (Kuhlemann et al., 2009; Žebre and Stepišnik, 2014, 2015; Temovski et al., 2018), Pyrenees (Delmas, 2015), Cantabrian range (Serrano et al., 2015). Alpine glaciers downloaded from https://booksite.elsevier.com/9780444534477/ and modified in the Italian side using updated reconstructions (Ravazzi et al., 2012; Monegato et al., 2017; Gianotti et al., 2015; Ivy-Ochs et al., 2018; Rossato et al., 2018). Major European and eastern European lakes and rivers after Toucanne et al. (2015) and Verheul et al. (2015), Adriatic lakes (Miko et al., 2017) and rivers simplified from Maselli et al. (2014). Italian rivers draining major ice lobes at the outlet of alpine valleys are indicated with solid blue lines, outlined lines are used for lower-order rivers. Aeolian sediments (yellow polygons) based on data from compilations by Haase et al. (2007); Italian loess from Zerboni et al. (2018).

Fig. 5 Spatial vegetation changes at fixed 5 ka yrs long time slices between 60 and 30 ka yrs cal BP. The selected taxa are grouped according to their ecology and climatic preferences. Eurythermic conifers (orange): sum of *Pinus* and *Juniperus*; Temperate forest (red): sum of deciduous *Quercus*, *Alnus*, *Fagus*, *Acer*, *Corylus*, *Carpinus*, *Fraxinus*, *Ulmus*, *Tilia* and *Salix*; Xerophytic taxa (dark blue): sum of *Artemisia* and Chenopodiaceae. Italian Peninsula sketch map shows sea level 70 m below the present-day coastline (courtesy by S. Ricci, University of Siena), based on the global sea-level curve by Waelbroeck et al. (2002), but lacking estimation of post-MIS3 sedimentary thickness and eustatic magnitude.

Fig. 6 Sketch map showing the position of the Palaeolithic sites documenting the Uluzzian culture: 1) Klissoura Cave (Stiner et al., 2007); 2) Kephalari Cave (Darlas and Psathi, 2016); 3) Crvena Stijena (Morley and Woodward, 2011); 4) Grotta del Cavallo (Moroni et al., 2018); 5) Grotta di Serra Cicora (Spennato 1981); 6) Grotta Mario Bernardini (Borzatti

von Löwenstern 1970); 7) Grotta di Uluzzo (Borzatti von Löwenstern 1965); 8) Grotta di Uluzzo C (Borzatti von Löwenstern 1966); 9) Grotta delle Veneri (Cremonesi, 1987); 10) Torre Testa (Moroni et al., 2018); 11) Falce del Viaggio (Moroni et al., 2018); 12) Foresta Umbra (Moroni et al., 2018); 13) Atella Basin (Moroni et al., 2018); 14) Castelcivita (Gambassini, 1997); 15) Grotta della Cala (Benini et al.,1997); 16) S. Pietro a Maida (Moroni et al., 2018); 17) Tornola (Moroni et al., 2018); 18) Colle Rotondo (Moroni et al., 2018); 19) Grotta della Fabbrica (Dini 2012); 20) Val Berretta (Moroni et al., 2018); 21) Poggio Calvello (Moroni et al., 2018); 22) S. Lucia I (Moroni et al., 2018); 23) Indicatore (Moroni et al., 2018); 24) Villa Ladronaia (Moroni et al., 2018); 25) Maroccone (Moroni et al., 2018); 26) Salviano (Moroni et al., 2018); 27) Podere Collina (Moroni et al., 2018); 28) Val di Cava (Moroni et al., 2018); 29) Casa ai Pini (Moroni et al., 2018); 30) San Romano (Moroni et al., 2018); 31) San Leonardo (Moroni et al., 2018); 32) Porcari (Moroni et al., 2018); 33) Riparo del Broion (Peresani et al., 2019); 34) Grotta Fumane (Peresani et al., 2016).

Fig. 7 Geographic distribution of the Campanian Ignimbrite (CI) distal tephra layer in terrestrial and marine records (red dots) and archaeological sites (yellow squares). On the right: Tenaghi Philippon paleoecological record showing the CI chronostratigraphic position. Selected pollen curves of % arboreal pollen (green) and temperate taxa (orange) between 30 and 60 ka are shown.

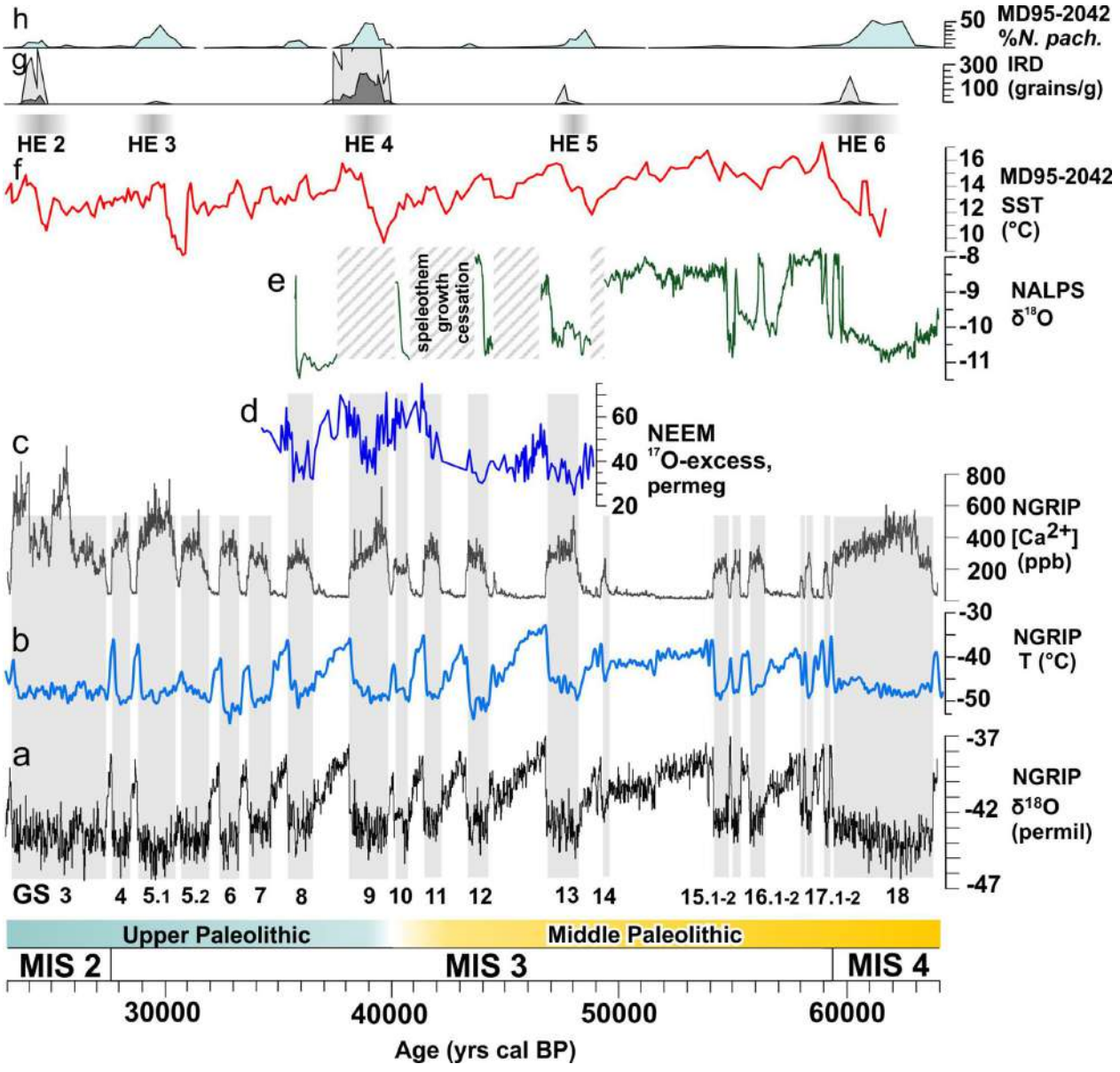
h
g
50
MD95-2042
%N. pach.
300
100
IRD
(grains/g)
HE 2
HE 3
HE 4
HE 5
HE 6
f
16
14
12
10
MD95-2042
SST
(°C)
e
speleothem growth cessation
-8
-9
-10
-11
NALPS
δ18O
d
60
40
20
NEEM
17O-excess,
permeg
c
800
600
400
200
NGRIP
[Ca2+]
(ppb)
b
-30
-40
-50
NGRIP
T (°C)
a
-37
-42
-47
NGRIP
δ18O
(permil)
GS 3 4 5.1 5.2 6 7 8 9 10 11 12 13 14 15.1-2 16.1-2 17.1-2 18
Upper Paleolithic
Middle Paleolithic
MIS 2
MIS 3
MIS 4
30000
40000
50000
60000
Age (yrs cal BP)

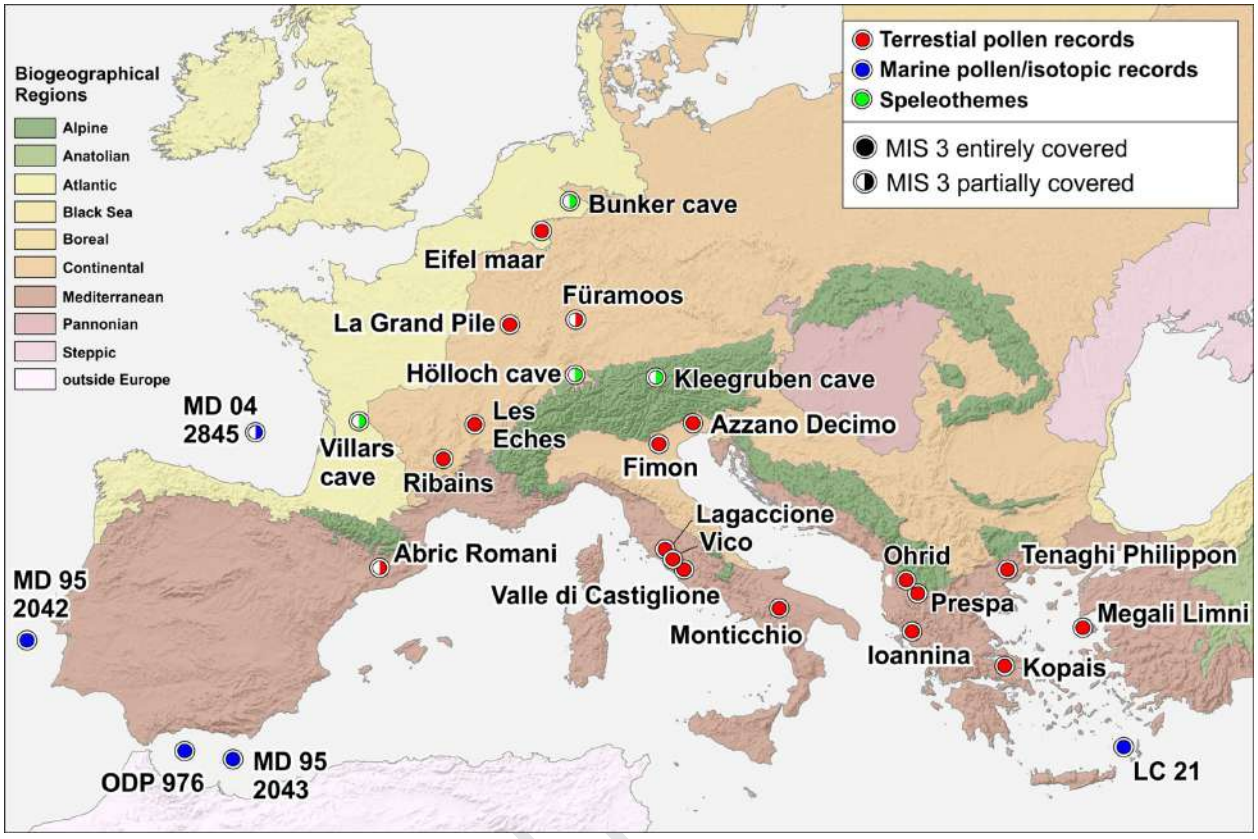

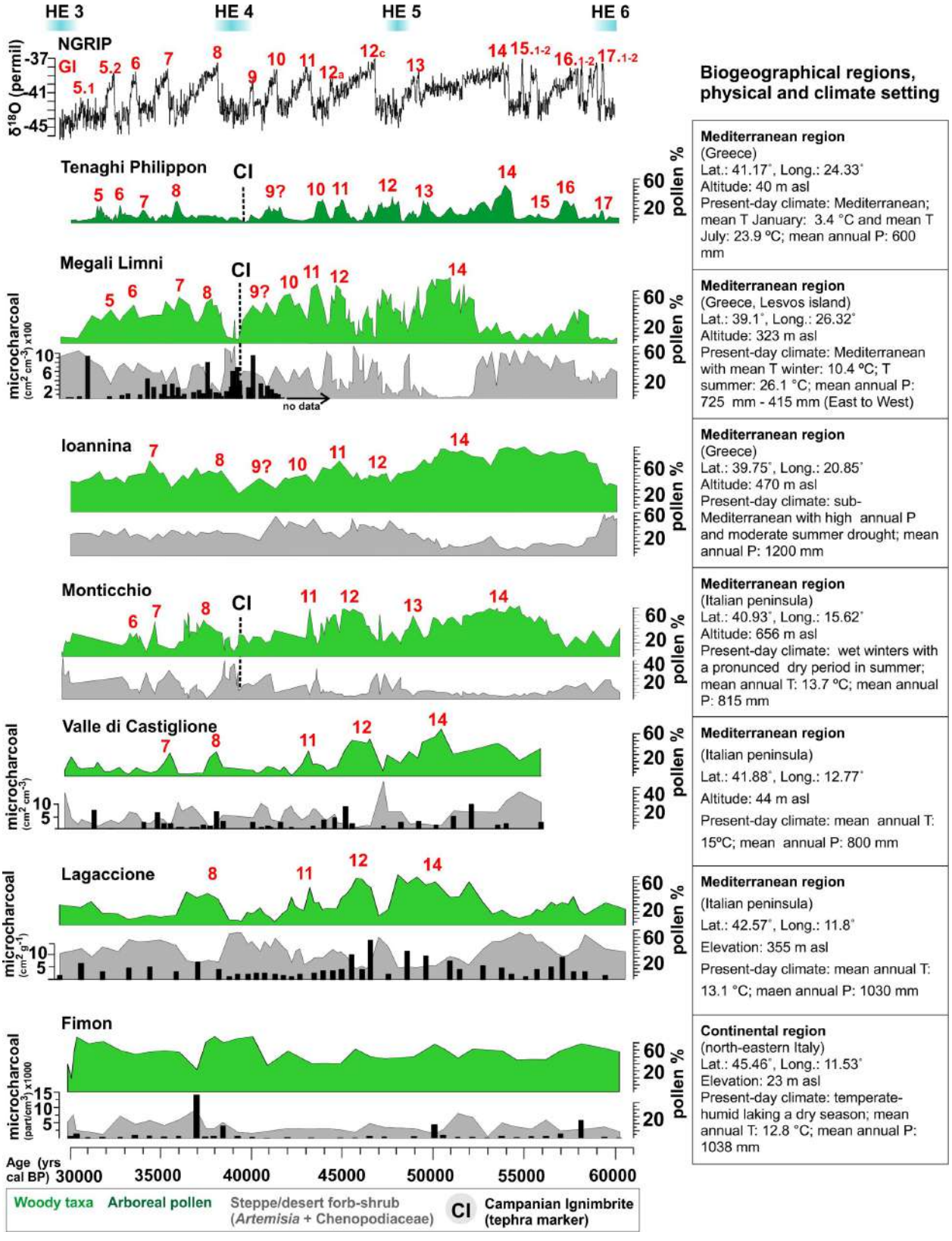

Biogeographical regions, physical and climate setting

Mediterranean region
(Greece)
Lat.: 41.17˚, Long.: 24.33˚
Altitude: 40 m asl
Present-day climate: Mediterranean; mean T January: 3.4 °C and mean T July: 23.9 ºC; mean annual P: 600 mm

Mediterranean region
(Greece, Lesvos island)
Lat.: 39.1˚, Long.: 26.32˚
Altitude: 323 m asl
Present-day climate: Mediterranean with mean T winter: 10.4 ºC; T summer: 26.1 °C; mean annual P: 725 mm - 415 mm (East to West)

Mediterranean region
(Greece)
Lat.: 39.75˚, Long.: 20.85˚
Altitude: 470 m asl
Present-day climate: sub-Mediterranean with high annual P and moderate summer drought; mean annual P: 1200 mm

Mediterranean region
(Italian peninsula)
Lat.: 40.93˚, Long.: 15.62˚
Altitude: 656 m asl
Present-day climate: wet winters with a pronunced dry period in summer; mean annual T: 13.7 ºC; mean annual P: 815 mm

Mediterranean region
(Italian peninsula)
Lat.: 41.88˚, Long.: 12.77˚
Altitude: 44 m asl
Present-day climate: mean annual T: 15ºC; mean annual P: 800 mm

Mediterranean region
(Italian peninsula)
Lat.: 42.57˚, Long.: 11.8˚
Elevation: 355 m asl
Present-day climate: mean annual T: 13.1 °C; maen annual P: 1030 mm

Continental region
(north-eastern Italy)
Lat.: 45.46˚, Long.: 11.53˚
Elevation: 23 m asl
Present-day climate: temperate-humid laking a dry season; mean annual T: 12.8 °C; mean annual P: 1038 mm


A
Reconstructed gradients ecogeography within eco-climatic zones
-74 500 1000 1500 2000 2500 Elevation m asl
Tundra zone
Forest - tundra zone (including Northern side of the Aps)
Southern side of the Alps
Tyrrhenian zone
Atlantic zone
Adriatic basin, Southern Balkan Peninsula and Circum-Aegean Area
Mid-Southern Iberian Peninsula
Central Anatolian Plateau
Glaciers
Major valley glaciers (Alps)
Freshwaters
Seawater
Sea level between -74 and -120 m
? ?
50°N
45°N
40°N
35°N
5°W
0°
5°E
10°E
15°E
0 125 250 500 750 1.000
Kilometers

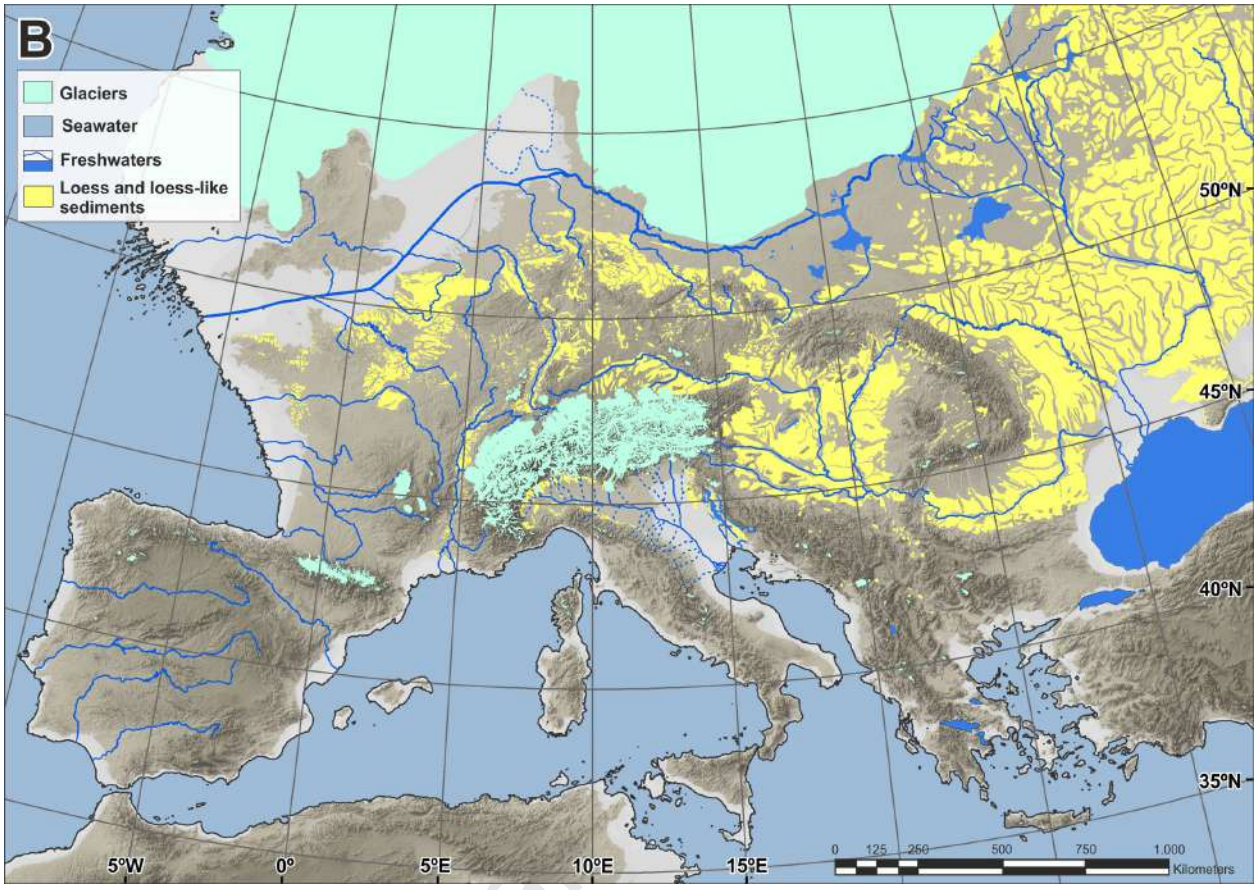
B
Glaciers
Seawater
Freshwaters
Loess and loess-like sediments
50°N
45°N
40°N
35°N
5°W
0°
5°E
10°E
15°E
0 125 250 500 750 1.000
Kilometers

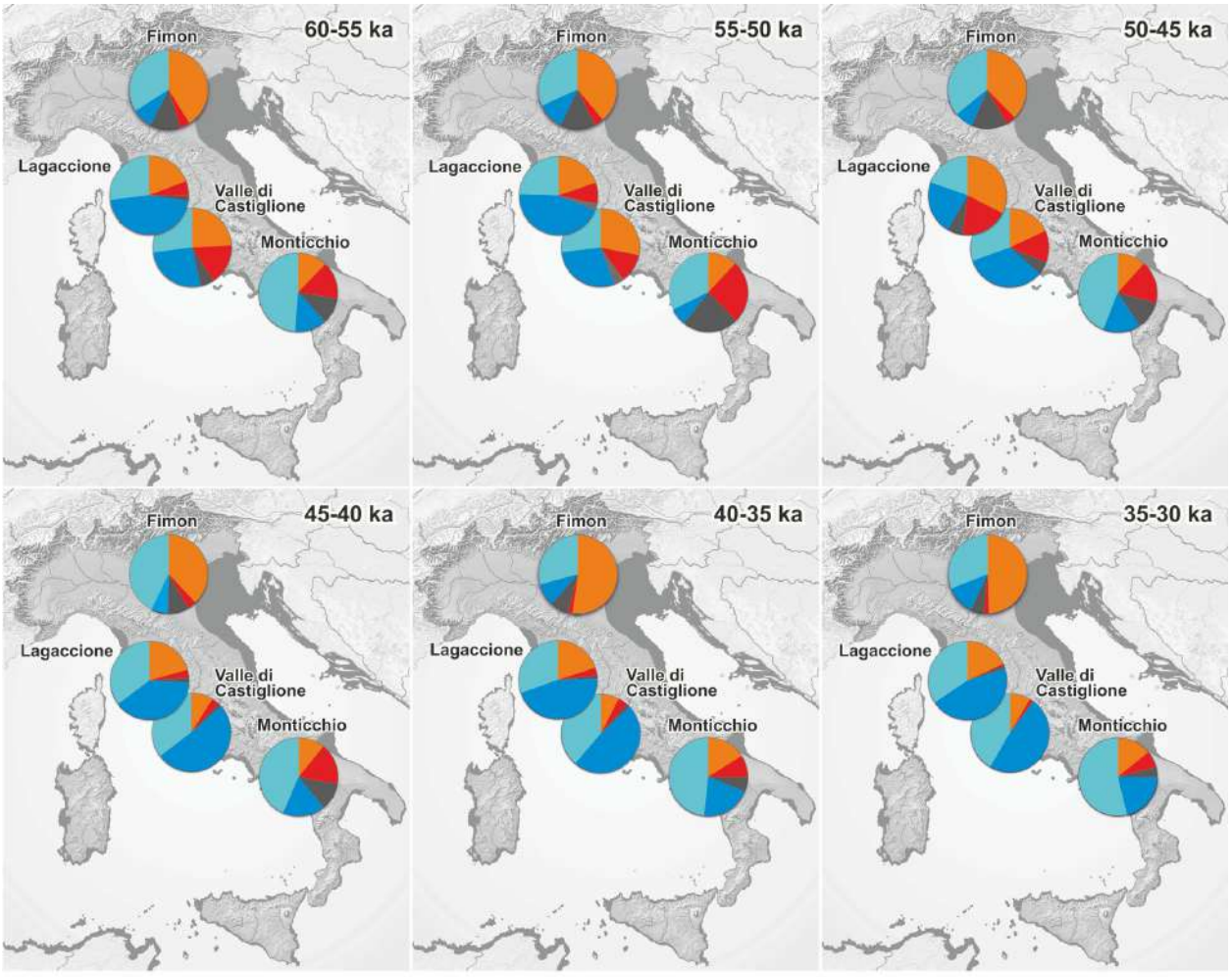
60-55 ka
55-50 ka
50-45 ka
45-40 ka
40-35 ka
35-30 ka
Fimon
Lagaccione
Valle di Castiglione
Monticchio
Legend:
Eurythermic conifers
Temperate forest
Other woody taxa
Xerophytic steppe
Other herbaceous taxa

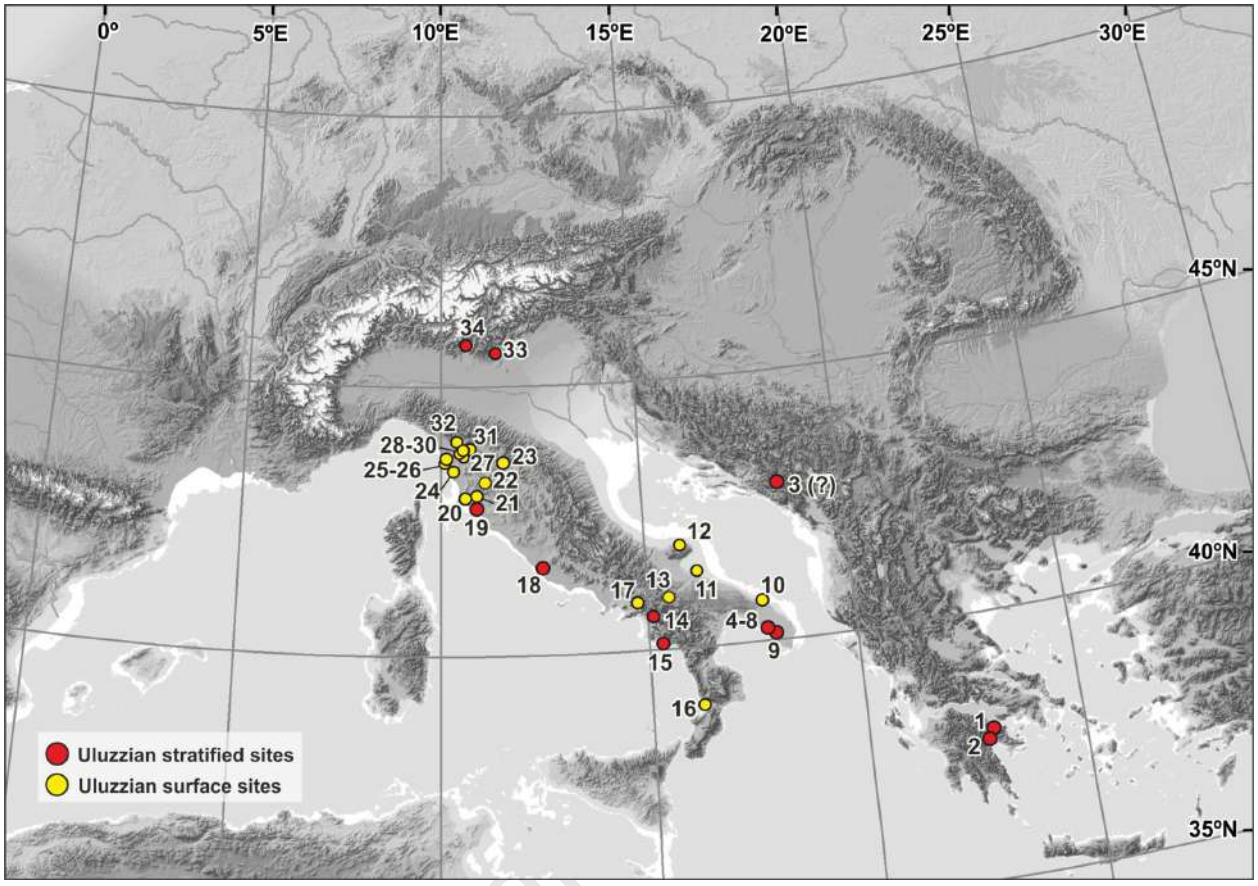
0°
5°E
10°E
15°E
20°E
25°E
30°E
45°N
40°N
35°N
34
33
32
31
28-30
27
23
25-26
22
24
21
20
19
3 (?)
12
18
17
13
11
10
14
4-8
9
15
16
1
2
Uluzzian stratified sites
Uluzzian surface sites

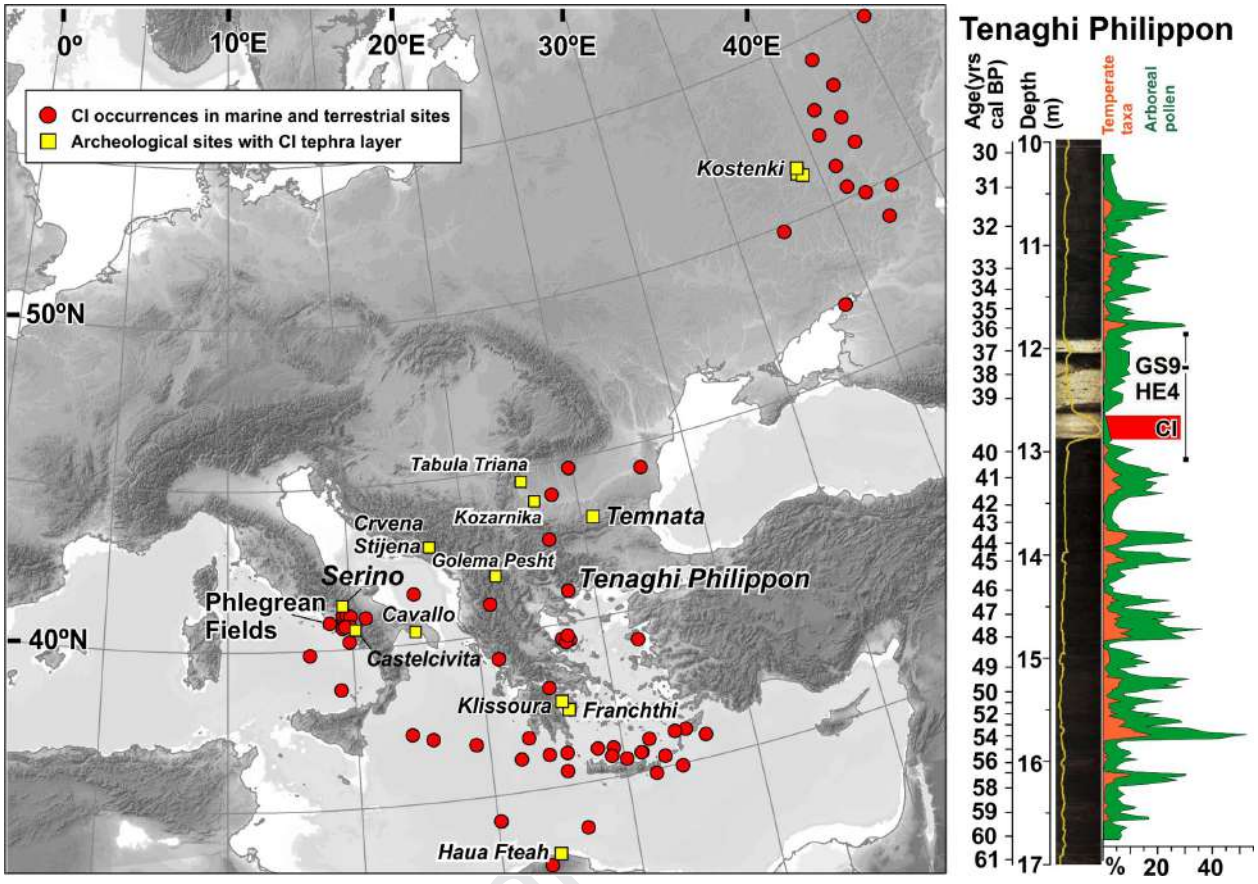
0º
10ºE
20ºE
30ºE
40ºE
50ºN
40ºN
CI occurrences in marine and terrestrial sites
Archeological sites with CI tephra layer
Kostenki
Tabula Triana
Kozarnika
Temnata
Crvena Stijena
Golema Pesht
Serino
Tenaghi Philippon
Phlegrean Fields
Cavallo
Castelcivita
Klissoura
Franchthi
Haua Fteah
Tenaghi Philippon
Age(yrs cal BP)
Depth (m)
Temperate taxa
Arboreal pollen
GS9-HE4
CI
%
20
40